ELEMENTA
Science of the Anthropocene

Darby, LS, et al. 2021. Spatial and temporal variability of ozone along the Colorado Front Range occurring over 2 days with contrasting wind flow. *Elem Sci Anth*, 9: 1. DOI: https://doi.org/10.1525/elementa.2020.00146

RESEARCH ARTICLE

# Spatial and temporal variability of ozone along the Colorado Front Range occurring over 2 days with contrasting wind flow

Lisa S. Darby[1,*], Christoph J. Senff[2,3], Raul J. Alvarez II[2], Robert M. Banta[2,3], Laura Bianco[1,3], Detlev Helmig[4], and Allen B. White[1]

Transport of pollution into pristine wilderness areas is of concern for both federal and state agencies. Assessing such transport in complex terrain is a challenge when relying solely on data from standard federal or state air quality monitoring networks because of the sparsity of network monitors beyond urban areas. During the Front Range air quality study, conducted in the summer of 2008 in the vicinity of Denver, CO, research-grade surface air quality data, vertical wind profiles and mixing heights obtained by radar wind profilers, and ozone profile data obtained by an airborne ozone differential absorption lidar augmented the local regulatory monitoring networks. Measurements from this study were taken on 2 successive days at the end of July 2008. On the first day, the prevailing winds were downslope westerly, advecting pollution to the east of the Front Range metropolitan areas. On this day, chemistry measurements at the mountain and foothills surface stations showed seasonal background ozone levels of approximately 55–68 ppbv (nmol $mol^{-1}$ by volume). The next day, upslope winds prevailed, advecting pollution from the Plains into the Rocky Mountains and across the Continental Divide. Mountain stations measured ozone values greater than 90 ppbv, comparable to, or greater than, nearby urban measurements. The measurements show the progression of the ozone-enriched air into the mountains and tie the westward intrusion into high-elevation mountain sites to the growth of the afternoon boundary layer. Thus, under deep upslope flow conditions, ozone-enriched air can be advected into wilderness areas of the Rocky Mountains. Our findings highlight a process that is likely to be an important ozone transport mechanism in mountainous terrain adjacent to ozone source areas when the right circumstances come together, namely a deep layer of light winds toward a mountain barrier coincident with a deep regional boundary layer.

**Keywords:** Colorado Front Range ozone, Ozone lidar, Upslope and downslope winds, Ozone transport

## 1. Introduction

On July 31, 2008, ground-level ozone mixing ratios reached 97 ppbv at a high-elevation (3,538 m mean sea level [MSL]) site south of Rocky Mountain National Park (RMNP), the highest value of the year. Ozone levels here exceed 90 ppb only a few times annually (e.g., 2 days in 2008). These high ozone concentrations are harmful to susceptible visitors to the National Park, to many delicate trees and other plant species, to animal wildlife from one-celled organisms to large mammals, and to the alpine ecosystems of which these plant and animal species are an integral part. High ozone levels were also measured at locations west of the Continental Divide in Northern Colorado, likewise mostly wilderness and rural locations.

Few significant local sources of ozone precursor emittants exist in high mountain areas and regions west of the Divide including the RMNP, so these pollutants must be imported. Studies have identified the Denver Metropolitan Area (DMA) as a major source of pollution in the region and have found that this pollution can be transported westward into and over the Rocky Mountains (Fehsenfeld et al., 1983; Sullivan et al., 2016; Pfister et al., 2017; Bien and Helmig, 2018; Flocke et al., 2019; Helmig, 2020). In RMNP, the Continental Divide is 2,150 m higher than the elevation of the city of Denver—a considerable barrier for an airmass to cross. Thus, important questions are, how do pollutants get up to and then over the Divide, and what meteorological conditions produce this transport?

The diurnal behavior of summertime winds in the mountains and adjacent plains of Northeastern Colorado have long been well known. Toth and Johnson (1985), for

[1] NOAA Physical Sciences Laboratory (PSL), Boulder, CO, USA
[2] NOAA Chemical Sciences Laboratory (CSL), Boulder, CO, USA
[3] Cooperative Institute for Research in Environmental Sciences (CIRES), University of Colorado Boulder, Boulder, CO, USA
[4] Boulder Atmosphere Innovation Research LLC, Boulder, CO, USA

* Corresponding author:
Email: lisadarbywx@gmail.com

example, composited surface mesonet data in this region by the time of day and found daytime easterly winds, which carry air toward and into the mountains. These diurnal flows represent upslope, upvalley, and ridge plains circulations generated by surface heating (Defant, 1951). Air chemistry studies, where pollutant species such as ozone, nitrogen oxides ($NO_x$), and certain volatile organic compounds (VOCs) species have been measured at high-elevation sites, have asserted that these diurnal "upslope" flows must be responsible for the transport of the pollutants to those locations. The assertions were based on the diurnal behavior and the mix of the chemical species detected, in many cases absent wind measurements (Fehsenfeld et al., 1983; Roberts et al., 1983; Brodin et al., 2010; Reddy and Pfister 2016; Letcher and Minder 2018; Helmig, 2020; Rossabi et al., n.d.).

Mechanisms have been proposed for transporting pollutants up and over a mountain barrier such as the Rocky Mountain Ranges. Low-level convergence can focus intense updrafts along and just downwind of a ridgeline (Banta 1984, 1986; Toth and Johnson, 1985; Bossert et al., 1989; Langford et al., 2010; Reddy and Pfister, 2016). In quiescent meteorological conditions, these flows have been hypothesized to recirculate pollutants, causing day-to-day increases in pollutant loading (Sullivan et al., 2016; Pfister et al., 2017). Pollutants can be carried into the mountains aloft, then mixed downward to the surface by turbulence caused by daytime heating or strong shear events. Under synoptic- or larger mesoscale easterly winds, pollutants can be directly advected over the mountains, especially when this flow is enhanced by daytime upslope and when the convective boundary layer over the region is deep enough.

Explaining the transport of pollutants that originate on the Plains to high-elevation sites and over the Divide requires more than invoking a generic "upslope" mechanism. Thermally forced flows toward the mountains occur on clear days when the gradient winds are not too strong—generally less than 10 m $s^{-1}$, which is the case during most summertime days in Northeastern Colorado. Yet, the appearance of pollutants at locations above 3,000 m MSL and areas to the west of the Divide is a rare event. It is important to document instances when such transport occurs and to identify how the pollutants made it to the high elevations. A key reason why this is important, beyond a basic understanding of the problem, is for numerical weather prediction model verification. Models evaluate our understanding of how the meteorological and chemical processes are integrated in producing observed conditions, and they are used to assess the potential effectiveness of proposed air quality mitigation strategies, for example, how to reduce the number of days when Class I areas such as RMNP suffer poor air quality. Accurately representing meteorological and air chemistry processes in the models is critical to having confidence in their results. Demonstrating this accuracy requires case studies of instances when transport to high elevations occurred, in which meteorological conditions are well-documented by measurements.

Documenting the important aspects of meteorological transport processes over complex terrain requires measuring the evolving vertical structure of the lower troposphere. In the present study, we use the National Oceanic and Atmospheric Administration/Chemical Sciences Laboratory's (NOAA/CSL) *T*unable *O*ptical *P*rofiler for *A*erosols and O*z*one (TOPAZ), an airborne ozone-sensing, differential absorption lidar, to continuously profile ozone concentrations along the flight track (Langford et al., 2009; Alvarez et al., 2011; Banta et al., 2013). We also employed three wind-profiling radars, two on the plains and the third, in the mountains, to provide hourly profiles of the winds and mixing depths. The airborne ozone lidar measured the depth or thickness of layers of ozone along the flight track, important for determining which transport mechanisms were operating. We combine these with more routine surface measurements of meteorology and air chemistry to give a clear picture of how the enhanced ozone was transported to the high mountain sites on July 31, 2008.

Vertical profiling and aircraft instrumentation were part of previous campaigns, undertaken to better understand air quality of the Rocky-Mountain's Northern Colorado Front Range (NCFR) region and the role of emissions from the newly expanded oil and natural gas industry as explained in Flocke et al. (2019). The aircraft made in situ measurements of many chemical species, providing a line of measurements at flight level along the flight track (Kaser et al., 2017; Pfister et al., 2017; Flocke et al., 2019). Profiles could be obtained during slant path missed approaches at airports, but these were not vertically oriented, and spirals take time to complete a somewhat-stacked vertical profile. Data from several kinds of ground-based profiling measurement systems on the Plains were also analyzed, including radar wind profilers (Sullivan et al., 2016), ground-based ozone lidars, one of which was a reconfiguration of the airborne ozone lidar used in this study (Alvarez et al., 2011; Sullivan et al., 2016), and tethered-balloon ozonesondes (Oltmans et al., 2019). Connections to mountain flows were made in ozone-lidar cross sections on the plains by Sullivan et al. (2016) who interpreted ozone in a layer 1,500–2,500 m above the surface as resulting from recirculation (other explanations also seem plausible). Oltmans et al. (2019) showed that ozone over the plains occupied a deep well-mixed layer, which they were able to relate to surface measurements at mountain locations.

The main goal of the Front Range Air Quality (FRAQ) study was to measure the transport of ozone into the mountains adjacent to the NCFR. In particular, we were interested in how far into the mountains the ozone could be transported and under what conditions it could be transported over the Continental Divide. We will show unequivocally that on July 31, 2008, the pairing of deep mixing depths with infrequently occurring deep easterly winds brought ozone-rich air (>90 ppbv) into the mountains and to Grand County, west of the Continental Divide. We use the previous day, July 30, as a contrast day to show the ozone transport pattern on a day dominated by downslope (westerly) winds, but with similar mixing depths.

The TOPAZ airborne lidar measurements in and near the Rocky Mountains presented here provide an unprecedented look at the ozone distribution in the NCFR and adjacent mountains. TOPAZ obtains ozone profiles at high spatial and temporal resolution, from aircraft flight level down to within 250 m of the ground, effectively mapping out the 3D distribution of ozone in the boundary layer and lower free troposphere. This capability is especially valuable in complex mountainous terrain because other means of measuring ozone aloft, such as airborne in situ observations, are unable to provide ozone data with the same vertical and horizontal coverage.

## 2. Background

RMNP is one of 12 federal mandatory Class 1 areas in Colorado. Class 1 areas are provided extra air quality and visibility protection through the Clean Air Act (42 U.S. Code § 7491). The State of Colorado is responsible for implementing this extra protection for Colorado Class 1 areas, which includes reducing emissions of the ozone precursors $NO_x$ and VOCs (Regional Haze State Implementation Plan, 2015). A complicating factor in the state's effort to protect RMNP is that the DMA and the NCFR have been designated to be in nonattainment of the ozone National Ambient Air Quality Standard (NAAQS) since 2012 (Bien and Helmig, 2018). This nonattainment area includes the portion of RMNP that lies east of the Continental Divide (Figure S1).

The DMA and NCFR have been plagued by poor air quality since at least the 1960s (Flocke et al., 2019), and thus, long-term air quality monitoring networks have been established to measure surface ozone in the DMA and NCFR, mostly by the State of Colorado and by NOAA. A rich history of scientific field campaigns in the region has enhanced understanding of the meteorology and chemistry that drive the distribution of pollution in the area (Flocke et al., 2019).

As research-grade air quality measurement platforms have evolved over the decades, so have the drivers of air pollution events along the NCFR (as documented in Flocke et al., 2019, and references therein) ranging from aerosols, ammonia from livestock, wood burning, and a variety of other industries. With tighter restrictions and subsequent reductions of $NO_x$ emissions came an increase in morning ozone minima in urban areas due to less nighttime destruction of ozone from reaction of NO associated with vehicle emissions (Bien and Helmig, 2018). In recent years, oil and gas exploration and extraction have increased to the northeast of the DMA, adding more VOCs and other pollutants into the air (Gilman et al., 2013; Pétron et al., 2014; McDuffie et al., 2016; Oltmans et al., 2019; Helmig, 2020). Recently, it has been found that the application of personal care products, such as shampoos and lotions, can contribute to air pollution along the Front Range (as well as other urban areas), with emissions of decamethylcyclopentasiloxane ($D_5$) comparable to vehicle emissions during rush hour in Boulder, CO (Coggon et al., 2018). All of this evolving chemistry has occurred against the backdrop of continuous population growth and urbanization.

The transport of ozone aloft and at the surface is further complicated by a source's proximity to complex terrain, as along the NCFR. The NCFR air quality is characterized by complex chemistry compounded by complex terrain. Despite changes in the composition of atmospheric pollutants along the NCFR over the decades, the local thermally driven transport mechanisms remain the same and understanding the meteorological drivers of both vertical and horizontal transport is key to understanding pollution events along the NCFR.

Our case study days are from 2008 when the NCFR was on the cusp of rapid growth of oil and gas exploration and drilling rig installations. Surface ozone has decreased in many areas throughout the United States as a result of stricter regulations and subsequent reductions of ozone precursor emissions. In the DMA and NCFR, however, a review of 2000–2015 data (a period that covers our case study days) found that maximum ozone values had not decreased as in other areas of the Western United States (Evans and Helmig, 2017; Bien and Helmig, 2018). Thus, despite successful pollution mitigation efforts in the DMA, poor air quality events continue to affect the NCFR due to the expansion of oil and gas activities in the region, accompanied by the continuing likelihood of transport into pristine mountain landscapes to the west.

### *2.1. Summertime ozone and meteorology along the Colorado Front Range*

More hours of sunlight on summer days lead to an increase in the photolysis of $NO_x$ and the oxidation of VOCs that work together to create ozone near the earth's surface in the boundary layer (Fehsenfeld et al., 1983; McDuffie et al., 2016; Cheadle et al., 2017). Many diverse sources of these compounds exist along the Front Range of Colorado that contribute to the production of summertime ozone in the DMA and NCFR (Gilman et al., 2013; Pétron et al., 2014; McDuffie et al., 2016; Flocke et al., 2019). However, the number and strength of these sources decreases rapidly in the elevated terrain between the metropolitan areas of Denver, Boulder, and Fort Collins and high-altitude locations such as RMNP (Rossabi et al., n.d.).

In complex terrain urban areas, a distinct diurnal cycle of pollution production and meteorology occurs under these summertime stagnant conditions. Early in the morning, emissions of $NO_x$ from rush hour traffic cause a reaction with ozone as vehicle emissions are trapped in the remnants of a shallow, stable nocturnal boundary layer, creating a loss of ozone. After sunrise, the shallow, previous night's nocturnal boundary layer begins to grow through convective mixing (Banta and Cotton, 1981), leading to entrainment of pollution from aloft into the developing boundary layer (Fehsenfeld et al., 1983; Stull, 1988; Kaser et al., 2017; Oltmans et al., 2019). In the NCFR, Kaser et al. (2017) found that early morning entrainment could account for a 5 ppbv/h increase in boundary layer ozone in the early morning. Oltmans et al. (2019) found entrainment from aloft to be the key process for midmorning ozone concentration increases as the boundary layer grows. They found that the ozone increased uniformly throughout the entire boundary layer in the late morning

and early afternoon. In the afternoon, Kaser et al. (2017) found that continued entrainment has a dilution effect, a reversal from the morning fumigation. They showed that dilution caused an average decrease of −1.4 ppbv/h of ozone in the boundary layer.

Vertical mixing occurs throughout the day as the boundary layer grows. The depth of the daytime boundary layer depends on meteorological conditions: clear skies, high daytime temperatures, and weak winds in the absence of strong synoptic-scale subsidence foster deeper boundary layers. These conditions also favor the production of ozone (White et al., 2007; Reddy and Pfister, 2016). After sunset, the boundary layer becomes stable, decreasing in depth as mixing at the surface is suppressed, generally leaving a reservoir of pollution aloft as the stable layer near the surface decouples from the free atmosphere (Stull, 1988). Local transport of ozone and its precursors also plays a role in determining observed ozone concentrations at a given site (Oltmans et al., 2019).

Summertime winds during clear sky and high surface pressure conditions on the plains near the Front Range follow a cycle as documented in Toth and Johnson (1985): downslope winds that drain into the South Platte River Valley during the night, the initiation of upslope winds along the foothills by 08:00 Mountain Standard Time (MST), with complete upslope flow dominating the region by 11:00 MST, and finally the transition back to downslope flows in the foothills beginning around 17:00 MST and continuing through the evening. The heating and cooling of the elevated terrain of the foothills drives the upslope and downslope winds, and the Cheyenne Ridge to the north of Fort Collins and the Palmer Divide to the south of Denver cause their own downslope and upslope flows, adding to the complexity of the regional wind flows. Specifically, in the northern part of our study area, downslope flows associated with the Cheyenne Ridge are northerly and, in the DMA, the downslope flows associated with the Palmer Divide are southerly.

During the morning and evening transitions between upslope and downslope flows, particularly along the Foothills, convergence zones form that can be focal points for vertical transport and even thunderstorm initiation (Banta, 1984; Toth and Johnson, 1985). These convergence zones are thus areas where pollution can be lofted upward, similar to what happens in a sea breeze convergence zone (Banta et al., 2005), or areas where pollutants can accumulate, which often happens at the foot of the Rockies (Colorado Air Quality Control Commission/Regional Air Quality Council, 2020). Afternoon thunderstorms and synoptic events such as cold fronts can interrupt the normal surface wind flow patterns, ushering polluted air upward or horizontally out of the DMA.

Smaller scale terrain-driven circulations, such as the Denver Cyclone (Szoke et al., 1984), may also form under synoptically quiescent conditions. The Denver Cyclone is a small-scale cyclonic vortex, the center of which occurs near downtown Denver under south or southeasterly synoptic flow. This feature has been associated with thunderstorm initiation and severe weather (Szoke et al., 1984), but it can also lead to the accumulation of pollutants in the DMA. The recirculation of pollutants during a Denver Cyclone episode was found to contribute to poor visibility during winter months, along with 500 hPa ridging and a lee trough to the east of Denver (Reddy et al., 1995). The presence of a Denver Cyclone may block drainage flows that would advect pollution out of the Denver Metro area. Diurnal winds driven by differential heating between the slopes of the Rocky Mountains and the plains to the east are often referred to as a mountain–plains circulation or solenoid flow. The resulting winds can transport ozone and its precursors toward the plains (downvalley) during nighttime downslope conditions and then back toward the mountains during daytime upslope conditions (Bossert et al., 1989; Reddy and Pfister, 2016; Sullivan et al., 2016; Letcher and Minder, 2018). This cycle could lead to enhanced levels of ozone if aged ozone and its precursors were recirculated and mixed with freshly produced pollution.

Brodin et al. (2010) assessed the seasonal and diurnal cycles of ozone measurements at the following surface ozone stations: TL, SD, C1, CO, SL, BE, SB, and BO (all used in our analysis, except for BO, **Figure 1**) from September 2007 through August 2008 (including our case study days). In general, Brodin et al. (2010) found that all of

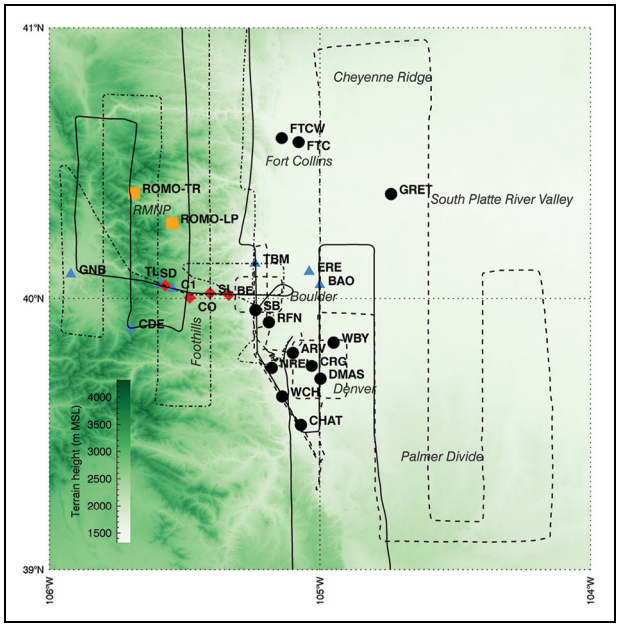


**Figure 1.** Map of the study area. Surface stations, flight tracks, CDPHE stations (black circles), RMNP stations (orange squares), NOAA stations (blue triangles), and CU stations (red diamonds). The dashed flight track is for the July 30, 2008, flight, the solid flight track is for the daytime flight on July 31, 2008, and the dash-dot track is for the evening flight on July 31, 2008. The shaded background is terrain in meters mean sea level. Station abbreviation codes are explained in **Table 1**. CDPHE = Colorado Department of Public Health and Environment; RMNP = Rocky Mountain National Park; NOAA = National Oceanic and Atmospheric Administration; CU = University of Colorado at Boulder. DOI: https://doi.org/10.1525/elementa.2020.00146.f1

these stations exhibited a diurnal cycle in the summer months, but the differences between the daytime ozone maxima and nighttime ozone minima were smaller at the higher elevations (e.g., 5 ppbv at TL vs. 29 ppbv at BO in the city of Boulder). Ozone measured at TL tended to reflect the background ozone of the region, without the spikes in the daily ozone seen in urban areas (Brodin et al., 2010). Bien and Helmig (2018) also show a smaller diurnal amplitude in rural ozone versus urban ozone.

The mid- to upper elevation stations were more likely to have similar afternoon ozone maxima in the spring and summer, whereas during the rest of the year, the daytime ozone maxima were more likely to be stratified by elevation, where ozone values increase with station elevation (see **figure 4** in Brodin et al., 2010). Boundary layer depth and vertical mixing (either upward from the source regions on the plains or downward from the stratosphere, especially in the spring, Langford et al., 2009; Brodin et al., 2010), play a role in this seasonal difference among the stations. During winter, when the boundary layer is shallower, the upper elevation stations mostly experienced background ozone, which is greater than what is typically measured at the urban stations during winter (Brodin et al., 2010). On hot summer days, the deeper, well-mixed boundary layer over the plains has greater concentrations of ozone and its precursors that are available for advection toward the mountains when easterly winds occur, which is a key element in our analysis. In a much earlier study of the diurnal cycle of ozone and its precursors at Niwot Ridge (C1, Fehsenfeld et al., 1983), the authors found that during the summer, increases in ozone were well-correlated with increases in $NO_x$ and other anthropogenic compounds. They interpreted these increases in ozone at C1 as in-transit photochemical production, so that it was the transport that drove the diurnal cycle of ozone at C1.

In this study, we provide a well-documented example of a pair of contrasting days that clearly show the role of transport and mixed-layer depth in the occurrence of large ozone concentrations in otherwise pristine mountain locations. The transport of ozone to the west from the plains to the mountains was directly tied to the growth of the afternoon boundary layer.

## 3. Experiment

### *3.1. Overview*

The FRAQ study was conducted in summer 2008 to investigate the complex transport patterns and the resulting distribution of ozone in the NCFR. The study was centered on the deployment of the NOAA/CSL airborne TOPAZ lidar (Alvarez et al., 2011), which was flown on a NOAA Twin Otter aircraft based out of the Rocky Mountain Metropolitan Airport in Broomfield, CO. From July 19 to 31, 2008, seven research flights were conducted. The objectives of these flights were to map out the ozone distribution in the NCFR and to test recent hardware upgrades of the TOPAZ lidar. The NOAA Physical Sciences Laboratory (PSL) added a small network of radar wind profilers and a surface meteorological station on the Continental Divide to the mix of instruments deployed during FRAQ. The University of Colorado at Boulder (CU) operated several in situ ozone sensors in the foothills and mountains above Boulder for a 15-month period that overlapped the FRAQ time window (Brodin et al., 2010). The routine surface ozone measurements from the NOAA Global Monitoring Laboratory (GML) and the Colorado Department of Public Health and Environment (CDPHE) provided the context of the FRAQ observations. Although limited in scope and duration, FRAQ nonetheless provided an important glimpse at the spatial distribution and transport patterns of ozone in the NCFR by bringing together a unique mix of research-grade and long-term, regulatory measurements.

### *3.2. Instrumentation*

**Table 1** lists the measurements used in the analyses and site locations, and **Figure 1** shows these locations, as well as flight tracks from the 2 days we analyzed in detail.

#### 3.2.1. Surface ozone and surface winds

The CDPHE maintains a long-term air quality monitoring network having many NCFR sites, including sites in or near the cities of Denver, Boulder, and Fort Collins (black circles in **Figure 1**). We requested quality-controlled data from the CDPHE; annual reports about the details of the CDPHE air quality measurements can be found at their web site (CDPHE, 2009). Here, we use hourly averages of ozone, wind speed, and wind direction from the CDPHE stations listed in **Table 1** and shown in **Figure 1**. Note that not all ozone measuring sites include wind measurements.

We analyzed meteorological and chemistry data from several Federal entities, as will be explained in greater detail below, some measurement stations were part of long-term measurement programs, and others were in place for the FRAQ study. The PSL deployed meteorological stations for FRAQ to the Continental Divide (CDE), to two sites east of the Foothills, Table Mountain (TBM) and Erie (ERE), and to a site west of the Divide at Granby (GNB). GNB, TBM, and ERE surface measurements were colocated with PSL radar wind profilers (described below). We used hourly averages of wind speed and direction from these surface meteorology sites (NOAA/Physical Sciences Laboratory, 2020).

The GML maintains long-term air chemistry monitoring stations at high elevations in Colorado at the Tundra Lab (TL) and Niwot Ridge (C1), represented by blue triangles in **Figure 1** (McClure-Begley et al., 2014; NOAA/Global Monitoring Laboratory, 2020). We used hourly averaged ozone measurements from these two stations as well as those from the GML Boulder Atmospheric Observatory (BAO) site on the plains. The National Park Service deploys high-altitude air quality monitoring sensors in RMNP: Trail Ridge Road (ROMO-TR) and Longs Peak (ROMO-LP, orange square symbols in **Figure 1**). We used hourly ozone averages and wind speed and direction to show the conditions at these sites.

For 15 months, starting in August 2007, researchers from CU Boulder deployed four ozone monitors along the slopes of the foothills west of Boulder, CO (Brodin et al., 2010). The sites, Betasso (BE), Sugarloaf (SL), Coughlin (CO), and Soddie (SD), are represented by red diamonds on **Figure 1**. These stations, as well as ones in Lyons, CO,

**Table 1.** Station identifier, latitude, longitude, station height, and station measurements analyzed in this article and funding agencies. DOI: https://doi.org/10.1525/elementa.2020.00146.t1

| Station | Latitude (°) | Longitude (°) | Elevation (m MSL) | Measurements Used | Supporting Agency |
|---|---|---|---|---|---|
| GRET | 40.39 | −104.74 | 1,482 | Ozone (UV absorption) | CDPHE |
| FTC | 40.58 | −105.08 | 1,523 | Ozone (UV absorption); surface winds | CDPHE |
| ERE | 40.10 | −105.04 | 1,530 | Mixing height (may add wind profile) | NOAA/PSL |
| WBY | 39.84 | −104.95 | 1,554 | Ozone (UV absorption); surface winds | CDPHE |
| FTCW | 40.59 | −105.14 | 1,569 | Ozone (UV absorption) | CDPHE |
| BAO | 40.05 | −105.00 | 1,579 | Ozone (UV absorption) | NOAA/GML |
| DMAS | 39.70 | −104.00 | 1,594 | Ozone (UV absorption); surface winds | CDPHE |
| CRG | 39.75 | −105.03 | 1,620 | Ozone (UV absorption); surface winds | CDPHE |
| ARV | 39.80 | −105.10 | 1,639 | Ozone (UV absorption); surface winds | CDPHE |
| SB | 39.96 | −105.24 | 1,670 | Ozone (UV absorption) | CDPHE |
| CHAT | 39.53 | −105.07 | 1,674 | Ozone (UV absorption); surface winds | CDPHE |
| TBM | 40.13 | −105.24 | 1,692 | Wind profile; surface winds; mixing height; ozone (UV absorption) | NOAA/PSL and CSL |
| WCH | 39.64 | −105.14 | 1,742 | Ozone (UV absorption); surface winds | CDPHE |
| RFN | 39.91 | −105.19 | 1,802 | Ozone (UV absorption); surface winds | CDPHE |
| NREL | 39.74 | −105.18 | 1,830 | Ozone (UV absorption) | CDPHE |
| BE | 40.01 | −105.34 | 1,943 | Ozone (UV absorption) | CU |
| SL | 40.02 | −105.41 | 2,399 | Ozone (UV absorption) | CU |
| GNB | 40.09 | −105.92 | 2,491 | Wind profile; surface winds; mixing height | NOAA/PSL |
| CO | 40.00 | −105.48 | 2,539 | Ozone (UV absorption) | CU |
| ROMO-LP | 40.28 | −105.55 | 2,741 | Ozone (UV absorption); surface winds | NPS |
| C1 | 40.04 | −105.54 | 3,035 | Ozone (UV absorption) | NOAA/GML |
| SD | 40.05 | −105.57 | 3,345 | Ozone (UV absorption) | CU |
| ROMO-TR | 40.39 | −105.69 | 3,488 | Ozone (UV absorption); surface winds | NPS |
| TL | 40.05 | −105.59 | 3,538 | Ozone (UV absorption) | NOAA/GML |
| CDE | 39.89 | −105.70 | 3,673 | Surface winds | NOAA/PSL |
| TOPAZ | Airborne | See **Figure 1** for flight tracks | | Ozone profiles | NOAA/CSL |

MSL = mean sea level; UV = ultraviolet; CDPHE = Colorado Department of Public Health and Environment; NOAA = National Oceanic and Atmospheric Administration; PSL = Physical Sciences Laboratory; GML = Global Monitoring Laboratory; CSL = Chemical Sciences Laboratory; CU = University of Colorado at Boulder; NPS = National Park Service.

and Longmont, CO (not shown), filled an important gap in measuring and understanding the upslope transport of pollution. The hourly averaged ozone from these sensors, combined with the GML sensors, provided an excellent source of ozone data along an approximately east/west line from an altitude of 1,943 m above MSL (BE) to 3,538 m MSL (TL). CU instrumentation and quality control measures are described in detail by Brodin et al. (2010). The precision of the hourly ozone values were estimated as <1 ppbv and the bias was found to be $\leq$1 ppbv. Throughout the article, we refer to this measurement array as the "slope array."

#### 3.2.2. Airborne ozone measurements

The TOPAZ lidar (Alvarez et al., 2011) measures profiles of ozone and aerosol backscatter at high spatial and temporal resolution. It incorporates modern solid-state laser technology; the laser transmitter is tunable in the ultraviolet spectral region. The system is lightweight and compact, so it can be flown on a rather small research aircraft such as the NOAA Twin Otter used here. In 2011, the TOPAZ lidar was reconfigured into a truck-based, uplooking system and was outfitted with an elevation-angle scanner (Alvarez et al., 2012). Prior to the ozone and aerosol backscatter retrieval, the TOPAZ data undergo a rigorous

quality control process, which includes corrections of signal biases due to electromagnetic signal interference and photomultiplier afterpulsing, and screening of erroneous signals due to hard target returns from cloud tops or the ground (Alvarez et al., 2011). In addition, data recorded during aircraft turns are discarded because the aircraft attitude information was not recorded. During FRAQ, seven research flights were flown totaling about 26 h. The aircraft typically flew at an altitude of about 5 km MSL. The downward-looking lidar provided profiles of ozone and aerosol backscatter along the flight track below the aircraft from 4,000 m MSL to approximately 250 m above ground level (AGL). The vertical resolution of the ozone measurements was 90 m, and the time resolution was 10 s, corresponding to a horizontal resolution along the flight track of about 700 m. At these resolutions, the precision of the ozone profile data is typically 5–15%, increasing with range, that is, the statistical errors in the ozone retrievals are highest close to the ground. If the signal-to-noise ratio (SNR) is very low, for example, due to strong lidar signal extinction caused by high atmospheric ozone concentrations and a high flight altitude AGL, the statistical errors of the near-surface ozone data can be as high as 30%. The ozone profile data are typically accurate to within 5% (Alvarez et al., 2011). The profiles of ozone presented in this article provide much more spatial information regarding the vertical distribution of ozone than the point in situ measurements of ozone obtained by research aircraft presented in other NCFR air quality papers (e.g., Pfister et al., 2017).

Each flight typically lasted 4–5 h and covered the midday through afternoon time period, except for the second flight on July 31, which began around sunset. The flights were designed to first map out the ozone distribution over the Denver–Boulder urban area and then follow the ozone plume as it was advected away from the urban area with the evolving winds. **Figure 1** shows the relevant portions of the flight tracks flown on July 30 (dashed lines) and July 31 (solid lines for the daytime flight and dash-dot lines for the night flight).

#### 3.2.3. Radar wind profilers and mixing depths

PSL deployed radar wind profilers to three sites: ERE, GNB, and TBM (locations represented by blue triangles in **Figure 1**). The radar wind profilers used in FRAQ are the 915-MHz boundary layer type described by Carter et al. (1995). They are designed to measure wind profiles from near the surface through the boundary layer and lower free troposphere depending on atmospheric conditions. When multiple wind profilers are deployed in a network, as in FRAQ, they can help document the horizontal transport of pollutants. Boundary layer depths were derived from the wind profiler data (with the methodology described below) and provide an indication of the maximum altitude to which pollution is mixed vertically. For FRAQ, the wind profilers were configured to operate with two vertical profiling modes: one with 60-m resolution from approximately 120 m AGL to approximately 2,300 m AGL, and one with 100-m resolution from approximately 120 m to approximately 4,000 m AGL. The 100-m mode also used pulse coding (Schmidt et al., 1979) to improve height coverage in weaker scattering regions. We present a blend of the data from both operational modes. The wind profiles were computed hourly on site using a consensus routine, transmitted to a data hub in PSL, and displayed in near-real time on the internet. The wind profile data were further quality controlled after the field program using an automated program and by visual inspection.

The mixing depths were estimated using reflectivity measurements from the three radar wind profilers. These profilers receive the electromagnetic signal backscattered by fluctuations in the water vapor and temperature fields of the atmosphere. The atmosphere's refractive index structure parameter, $C_n^2$ is proportional to the radar signal return (SNR). White (1993) showed that regions of strong signal return are associated with the inversion that caps the convective boundary layer.

Hourly convective mixing depths were calculated using the automated objective algorithm of Bianco et al. (2008) that incorporates information on the returned SNR, variance of the vertical velocity, and spectral width of the vertical velocity; this information defines the mixing depth. The accuracy of the calculated mixing depths is within $\pm 120$ m (the width of two range gates). This is a conservative estimate since the automated estimations were also visually edited to eliminate potential outliers (Bianco et al., 2008). The mixing depth measurements presented in this article are key to understanding the transport of ozone to the high-altitude stations. Previously, White et al. (2007) showed the importance of mixing depths in New England high ozone events and state that vertical mixing is one of the most important processes in pollution transport. The TOPAZ ozone lidar data and the PSL profiler data, along with the co-located surface meteorology data, are unique to this FRAQ study and have not been previously presented in the peer-reviewed literature.

## 4. Case study days — July 30 and 31, 2008

### *4.1. Time series overview*

Time series of data from select stations (**Figure 2**) provide a time line for our two case study days (July 30 and 31, 2008). We refer to time in MST because ozone behavior and meteorology—photochemical production of ozone and thermally driven flows in complex terrain—are strongly tied to the diurnal cycle.

**Figure 2** shows ozone time series for four stations at different heights MSL (station heights are indicated on the right-hand *y*-axis by black squares), mixing depths from the ERE profiler (red diamonds), and the surface winds from the Continental Divide ([CDE] station, wind barbs at the top of the plot) for both July 30 and July 31. The ozone time-series data are from a Denver metropolitan station (DMAS, green line), two high-elevation stations (TL, black line, and C1, purple line), and a slope station in between (SL, blue line; see **Figure 1** for location of the stations).

The DMAS time series (green line) represents a typical urban summertime diurnal range of ozone. On July 30, we see the larger ozone diurnal cycle in Denver, reaching a 60

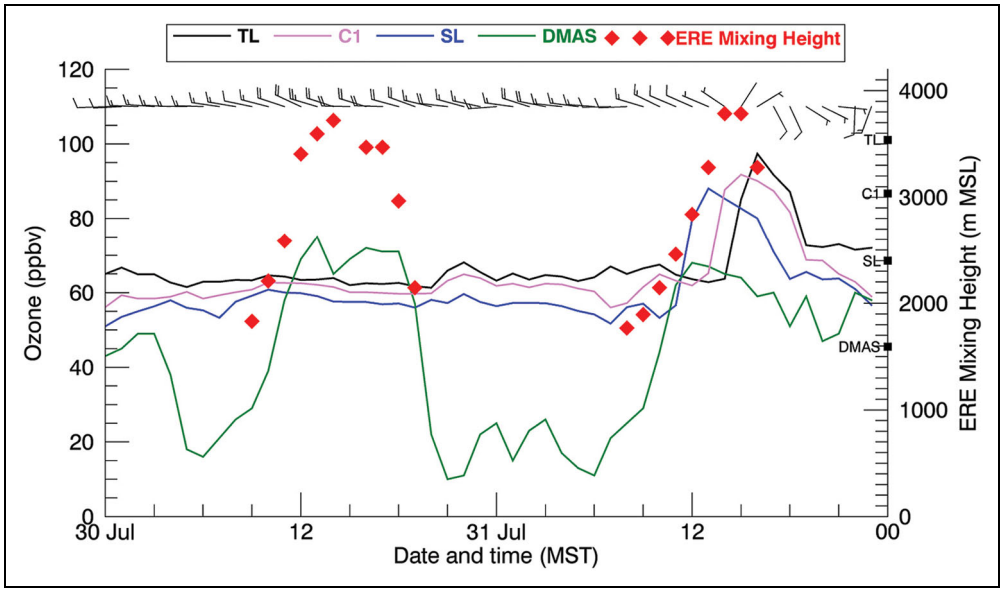


**Figure 2.** Time series of hourly surface-measured ozone at four surface stations: TL, C1, SL, and DMAS. The station heights are noted on the right *y*-axis by black squares. The red diamonds indicate mixing depths derived from the ERE radar wind profiler measurements as explained in the text. Along the top of the plot are surface wind barbs from the Continental Divide meteorological station CDE. The wind barbs are half barb = 2.5 m $s^{-1}$ and full barb = 5 m $s^{-1}$. DOI: https://doi.org/10.1525/elementa.2020.00146.f2

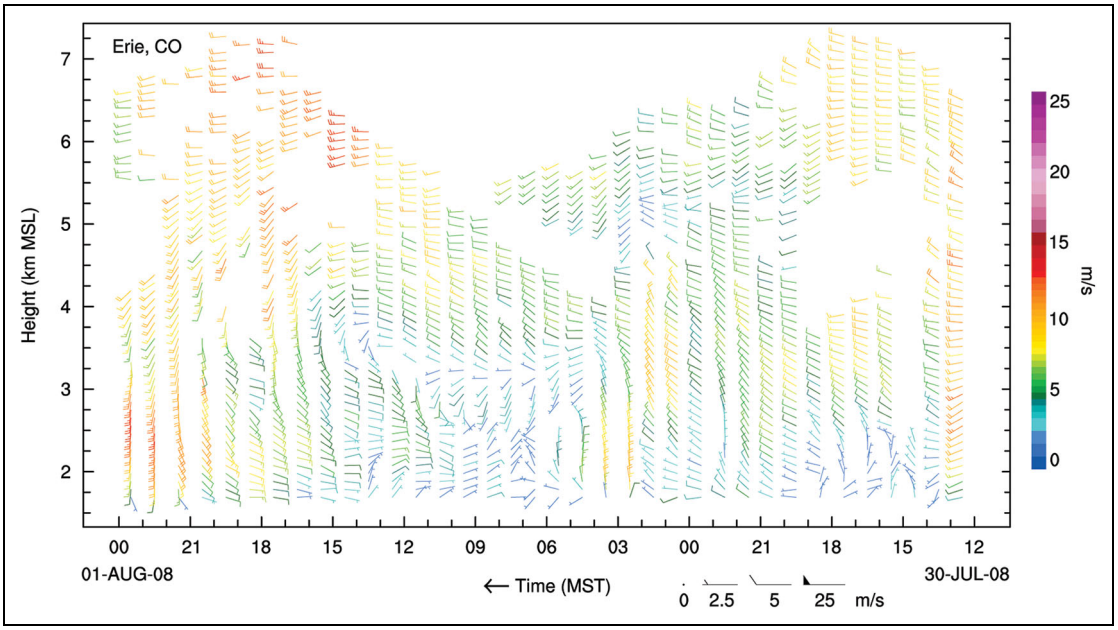


**Figure 3.** Radar wind profiler data from ERE. Data show the evolution of the winds on the plains throughout our two case study days. Wind profiles are hourly averages of the wind (m $s^{-1}$), arranged with time moving from right to left. The traditional wind barbs indicate wind direction and speed (as indicated in the key below the plot) and are also color-coded by wind speed. The growth of the easterly upslope flow is clearly shown in the July 31 profiles. DOI: https://doi.org/10.1525/elementa.2020.00146.f3

ppbv maximum-to-minimum difference, compared to that at the elevated stations, where the ozone remained relatively stable throughout the 24 h (consistent with diurnal cycles shown in Brodin et al., 2010, and Bien and Helmig, 2018). The mixed layer over the plains became quite deep, with a maximum of 3,721 m MSL. However, the upper level winds, as represented by the CDE surface winds (**Figure 2**) and radar wind profiler winds at 3,500 m MSL (**Figure 3**), remained westerly to northwesterly throughout the day.

On July 31, the morning ozone and ERE mixing depths were similar to those of July 30. As the mixing depth surpassed the station height of the slope and mountain stations, however, the surface ozone at these stations rapidly increased, exceeding measurements on July 30 by 27

ppbv at SL and C1, and 29 ppbv at TL, and for the entire year at C1 (Figure S2, data downloaded from NOAA/Global Monitoring Laboratory, 2020). The main meteorological difference between the 2 days was the wind direction at mountaintop height, as seen in the mountain surface station CDE wind measurements (**Figure 2**). On July 31, the winds shifted to easterly, not just at mountaintop level but through a deep layer, as seen in the wind profiler data. **Figure 3** shows a growing layer of easterly flow after 07:00 MST, reaching a depth of 3,500 m by 19:00 MST.

In the following sections, we further analyze surface ozone and wind measurements, wind profiles, and mixing depths using sequences of plan view and longitude height plots that show the ozone distribution and transport. The TOPAZ airborne ozone lidar measurements will reveal the horizontal and vertical spatial distribution of the ozone on these two case study days. TOPAZ measurements will confirm that a deep layer of ozone-rich air was available for advection to the mountain stations by the easterly winds on July 31.

### *4.2. Airborne ozone lidar measurements*

An overview of the airborne ozone lidar measurements for July 30 and 31 is shown in **Figure 4**. The observed ozone profiles are shown as "curtains" along the flight track and are overlaid on a Google Earth map of the NCFR. On July 30 (**Figure 4a**), fairly high ozone values of 75–100 ppbv were observed primarily to the east of the DMA in response to the westerly winds on that day. Greater ozone values were also found south of the DMA, whereas the Boulder and Fort Collins areas were quite clean with ozone values generally below 70 ppbv. On July 31 (**Figure 4b and c**), a day with easterly upslope winds, the ozone distribution was reversed compared to July 30: moderate ozone values (generally below 80 ppbv) were observed over the DMA, whereas the greatest ozone mole fractions in excess of 100 ppbv were measured in the Foothills northwest of Boulder and over the Rocky Mountains. The easterly flow advected ozone and its precursors from the DMA toward Boulder and farther west into the Front Range Mountains. During transport, photochemical production of ozone occurred, leading to the greater ozone values over the mountains to the northwest of Denver rather than over Denver and Boulder on the plains.

July 30, 2008, was dominated by a pressure ridge at 500 hPa, the center of high pressure sitting over Arizona, to the SW of Colorado (**Figure 5a**, National Centers for Environmental Prediction/National Center for Atmospheric Research reanalysis, Kalnay et al., 1996). The pressure gradient supported winds aloft having a westerly component over Colorado. As seen in the wind profiler data (**Figure 3**), the westerly winds extended from the surface to the top of the profiles and occurred throughout most of day. The 700 hPa plot (**Figure 5b**) showed a trough in Eastern Colorado and Western Kansas, further enhancing the west-to-east pressure gradient. The lee-side trough was also analyzed on July 30 synoptic surface maps (not shown).

By July 31, the 500-hPa ridge had expanded eastward, leading to a weaker pressure gradient across Colorado, especially at latitude 40°N, which slices through our area of interest (**Figure 5c**). The 700 hPa geopotential heights (**Figure 5d**) also showed a significant weakening of the pressure gradient across the state and an eastward drift of the pressure pattern; 700 hPa is approximately mountaintop height for the NCFR region. An analysis (not shown) of radiosonde data from Grand Junction (GJT), in Western Colorado, and Denver (DEN) showed that the geopotential height difference (GJT minus DEN) at 700 hPa was 13 m in the afternoon of July 30 and −2 m on the afternoon of July 31—indicating a reversal in the pressure gradient in the late afternoon that supported deep westerly winds up to mountaintop height on July 30 versus deep easterly winds on July 31. With the weaker pressure gradient aloft and the large-scale trough moving eastward, the synoptic meteorology had less influence over Eastern Colorado weather on July 31. The local-scale meteorology dominated, including the development of thermally driven flows. Both days were hot—the maximum temperature in Denver on July 30 was 37.2 °C and on July 31 was 35.6 °C.

### *4.3. Surface-based and airborne ozone lidar measurements combined*

To create an integrated visual of surface-based measurements with the TOPAZ measurements, we have created plan view maps that show hourly averaged surface ozone and surface winds, along with plots of vertically averaged ozone calculated from TOPAZ profiles obtained during the hour over which the surface ozone and winds were averaged. The vertical averages were calculated from all good data points from the bottom of each measurement profile up to 4,000 m MSL, and we plotted these averages along the flight track. We also show a subset of these surface stations plotted in a height versus longitude format to give a perspective on the ozone differences with height and time during our case study days. The height versus longitude plots also include horizontally averaged ozone profiles taken from flight legs flown during the hour over which the surface ozone and winds were averaged, wind profile data from two of the PSL wind profilers (TBM and GNB), and mixing depths derived from wind profiler data, when available. TBM wind profiles show the winds over the plains, near the foothills of the NCFR, whereas winds at GNB represent flow over Middle Park in the Rocky Mountains, west of the Continental Divide. For the horizontally averaged TOPAZ ozone profiles shown in the height–longitude plots, we only averaged over the sections of each leg that fell between the latitudes of DMAS and ROMO-TR. Consequently, the height–longitude plots may not include all TOPAZ data seen in the plan view plots. Also, to reduce clutter in the height–longitude plots, if two or more legs were flown along nearly the same longitude line, only the profile from the longest leg of the hour near that longitude was plotted.

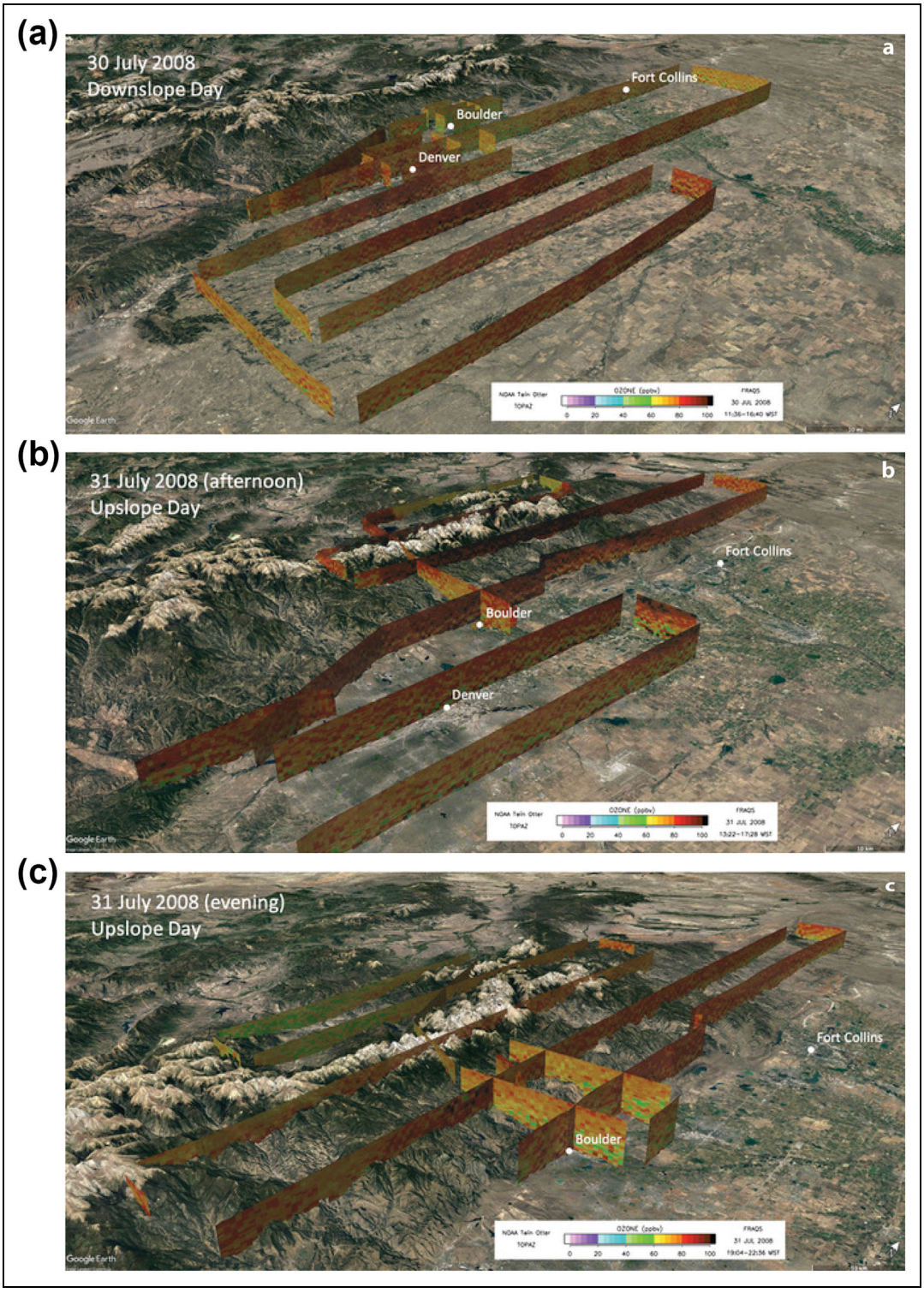


**Figure 4.** "Curtain" of ozone mole fraction profiles (ppbv) from the nadir-looking airborne TOPAZ lidar. Plots are overlaid over a Google Earth map of the NCFR and viewed from the southeast. (a) shows ozone profile data for the flight on July 30 (11:36–16:40 MST); (b) shows ozone profile data for the first flight on July 31 (13:22–17:28 MST); (c) shows ozone profile data for the evening flight (19:04–22:36 MST). Ozone profiles from all flights extend from 4,000 m mean sea level down to approximately 250 m above ground level. TOPAZ = *T*unable *O*ptical *P*rofiler for *A*erosols and Ozone; NCFR = Northern Colorado Front Range; MST = Mountain Standard Time. DOI: https://doi.org/10.1525/elementa.2020.00146.f4

#### 4.3.1. July 30

During the first hour of the TOPAZ afternoon flight (noon to 13:00 MST), the plan view plot of surface ozone measurements (**Figure 6a**) showed greater ozone mole fractions in the DMA (the stations south of 40°N, near longitude −105.0) than the rest of the network. In **Figure 6b**, the TOPAZ ozone profile averaged along −105° longitude over the DMA had a maximum ozone

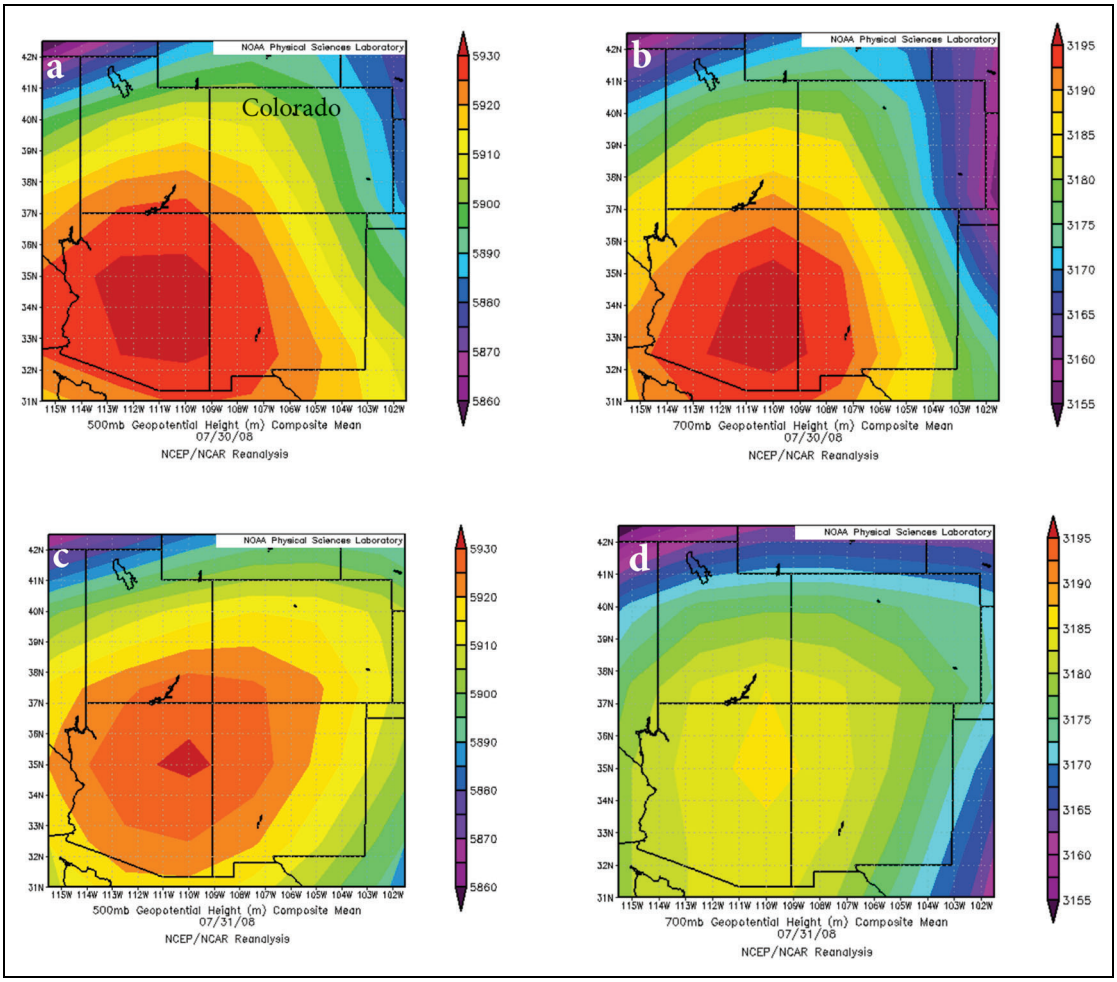


**Figure 5.** National Centers for Environmental Prediction/National Center for Atmospheric Research reanalysis 500 hPa and 700 hPa plots for July 30 and 31, 2008. Daily composite mean of the geopotential heights (m) for the constant pressure surfaces 500 and 700 hPa. This includes 00 Universal Time Coordinated (UTC) and 12 UTC reanalysis output for each day. (a) 500-hPa map for July 30, (b) 700-hPa map for July 30, (c) 500-hPa map for July 31, (d) 700-hPa map for July 31. DOI: https://doi.org/10.1525/elementa.2020.00146.f5

value of 83 ppbv and an average ozone value of 70 ppbv, while 70 ppbv was measured at the DMAS surface station over the hour, consistent with the TOPAZ profile average. The mixing height at ERE, indicated by the blue diamond on **Figure 6b**, was 3,600 m MSL. The mountain station ozone measurements (**Figure 6a and b**) indicated approximately background ozone levels, which are between 51.0 and 68.8 ppbv at TL in the summer (as determined by Brodin et al., 2010, see their table 2 for additional station background levels). The TBM profiler measurements for the next hour (not shown) indicated low-level easterly upslope flow 900 m deep. Thus, thermally forced mountain upslope flow did occur on this day, but it lasted only 1 h and was ineffective in transporting ozone into the foothills. Banta (1986) found from modeling and observational evidence that stronger ridgetop winds, as here, produce weaker, more disorganized, shorter lived daytime upslope winds than when the winds aloft are weaker. The foothills stations continued to measure background ozone during this hour (not shown).

Hourly averaged surface winds at 15:00 MST (**Figure 7a**) showed light and variable winds on the plains. Such light winds had been occurring and continued to occur throughout the afternoon, with no discernable pattern to provide consistent advection of pollution out of the DMA, at the surface. Mountain surface stations continued to show westerly winds throughout the afternoon and background ozone levels.

TOPAZ flight legs from 14:00 to 15:00 MST indicated ozone up to 100 ppbv well to the east of the DMA where there are no surface ozone monitors (**Figure 7a and b**), with ozone averages across each leg ranging from 63 to 78 ppbv, and maximum ozone values per leg ranged from 73 to 101 ppbv. The profiler data indicated deep westerlies throughout the profile, presumably advecting the elevated ozone-rich air to the eastern plains of CO throughout a deep layer, while the mountain stations continued to measure background ozone, showing that the mountain areas were not impacted by the urban ozone at this time.

From 16:00 MST to 17:00 MST (**Figure 8a and b**), TOPAZ obtained ozone profiles over and around the DMA

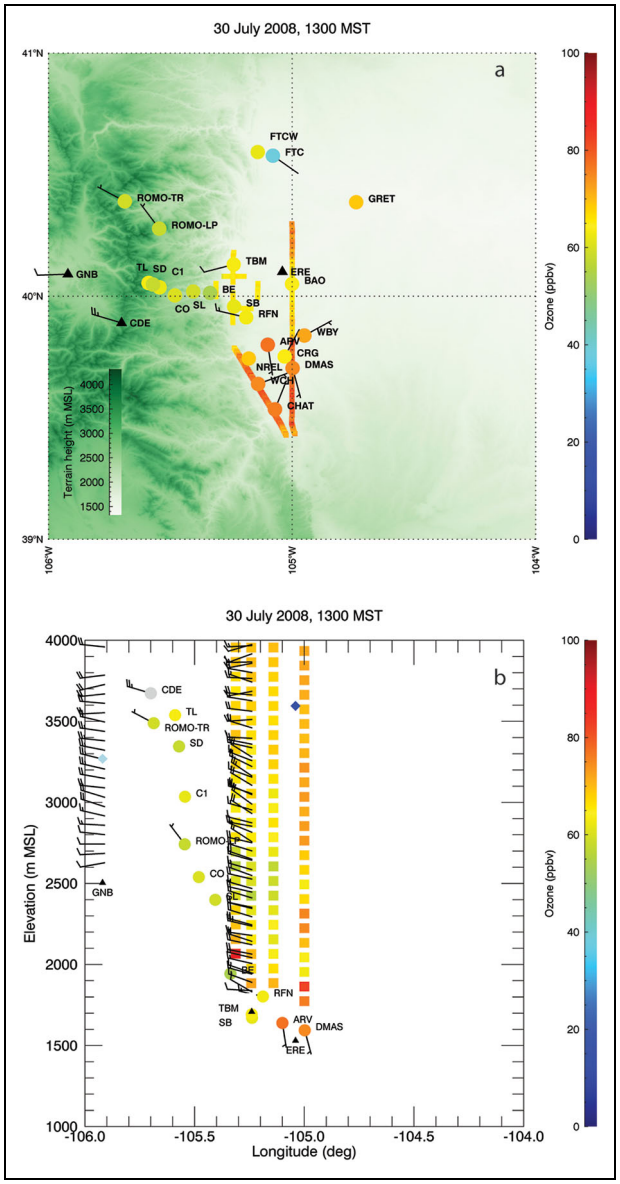


**Figure 6.** Plan view and height–longitude plots of hourly averaged ozone and winds. (a) The plan view plot shows hourly averaged winds and ozone measured at the surface, and vertical averages of airborne ozone lidar profiles along the flight tracks flown during the hour that matched the surface measurement hourly averages for July 30, 2008, 13:00 MST. Vertical averages of lidar data were performed on all good data points between the bottom of each TOPAZ profile and 4,000-m mean sea level. The station circles represent hourly averaged ozone. If the station circle is gray, then either ozone was not measured at the station or the hourly averaged ozone value was missing for that hour. The wind barbs are half barb = 2.5 m $s^{-1}$ and full barb = 5 m $s^{-1}$. (b) Height–longitude plot of select stations seen in the plan view plot of the same time showing surface ozone and wind measurements, wind profiles, mixing depths (blue diamonds), and vertical profiles of horizontally averaged ozone along each flight leg that occurred in the previous hour. The horizontal averaging of the profiles occurred only for the sections of each leg that fell between the latitudes of DMAS and ROMO-TR. Therefore, the height–longitude plot may not include all TOPAZ data seen in the corresponding plan view plot. The wind barbs are half barb = 2.5 m $s^{-1}$ and full barb = 5 m $s^{-1}$. TOPAZ = *T*unable *O*ptical *P*rofiler for *A*erosols and *O*zone; MST = Mountain Standard Time. DOI: https://doi.org/10.1525/elementa.2020.00146.f6

and along the foothills to the west and southwest of Denver, similar to the track flown from 12:00 to 13:00 MST (**Figure 6a**). TOPAZ-measured ozone averaged from 66 to 77 ppbv per flight leg, with maximum ozone from each leg ranging from 77 to 94 ppbv, greater than the maximum ozone measured at 13:00 MST. With DMA surface stations measuring ozone in the 60s and 70s, the TOPAZ-measured ozone was comparable when looking at the averages across the flight legs, but the maximum ozone measured aloft far exceeded what was measured at the ground. Mixing depths over the plains continued to remain deep (e.g., 3,469 m MSL at ERE), and winds at the mountain surface stations and in the PSL wind profiler data (**Figure 3**) continued to be dominated by westerly flow. Mountain station surface winds were 260°–285°, <4 m $s^{-1}$, except at the CDE station where winds were >10 m $s^{-1}$. The deep layer of enhanced ozone measured over the urban area is a reminder that a significant reservoir of ozone, and its precursors, could remain above the surface, available for both horizontal and vertical transport (Banta et al., 2005). Variation in the ozone measurements along each profile was small, indicating the measured ozone was fairly well mixed in the vertical.

### 4.3.2. July 31

At midnight MST on July 31 (Figure S3a), the nighttime surface winds were southerly (150°–210° at 0.25–1.5 m $s^{-1}$) at CHAT, DMAS, CRG, and WBY and 245°–305° at 1–7.5 m $s^{-1}$ (downslope) at the mountain and foothills stations (excluding GNB), consistent with the typical nighttime drainage winds described in Toth and Johnson (1985). Ozone dropped to <65 ppbv throughout the network, with ozone at the mountain stations at least 20 ppbv greater than at the plains stations, due to a lack of reaction with nitric oxide as a loss mechanism. At 06:00 MST (Figure S3b), the lowest ozone values (2–26 ppbv) occurred at the DMA urban stations ARV, CRG, DMAS, WCH, and WBY (as well as a low value at FTC in Fort Collins), most likely a result of reaction associated with nighttime nitric oxide emissions and morning traffic. By 09:00 MST (Figure S4a), upslope flow ranging from 60° to 165° and 1 to 6.5 m $s^{-1}$ had begun at surface stations near the foothills, such as TBM and RFN and in the DMA, because of mountain slope heating and the reversal of the larger scale east-west pressure gradient previously described. The longitude–height plot for the same time shows our first mixing depths at the profiler sites for the day (blue diamonds, Figure S4b).

The 13:00 MST plan view and longitude–height plots (**Figure 9a and b**) showed greater amounts of ozone at the slope stations and at ROMO-LP, in RMNP, in contrast to the background amounts of ozone seen at the slope and mountain stations at the same hour on the previous day

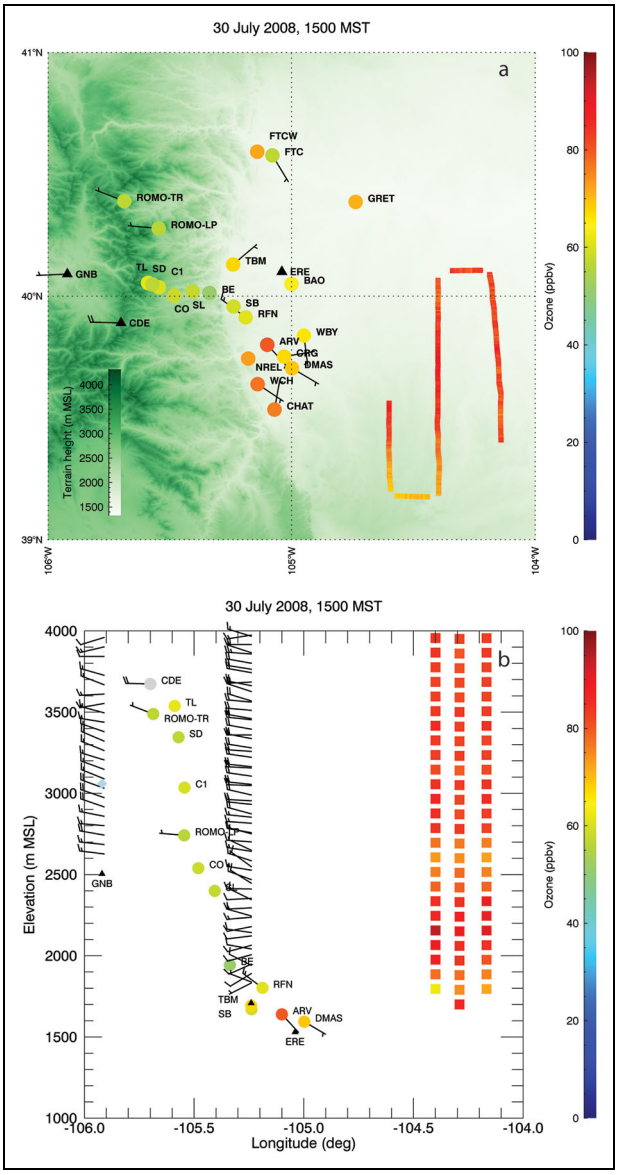


**Figure 7.** Plan view and height–longitude plots of hourly averaged ozone and winds. Same as **Figure 6** except for July 30 at 15:00 MST. DOI: https://doi.org/10.1525/elementa.2020.00146.f7

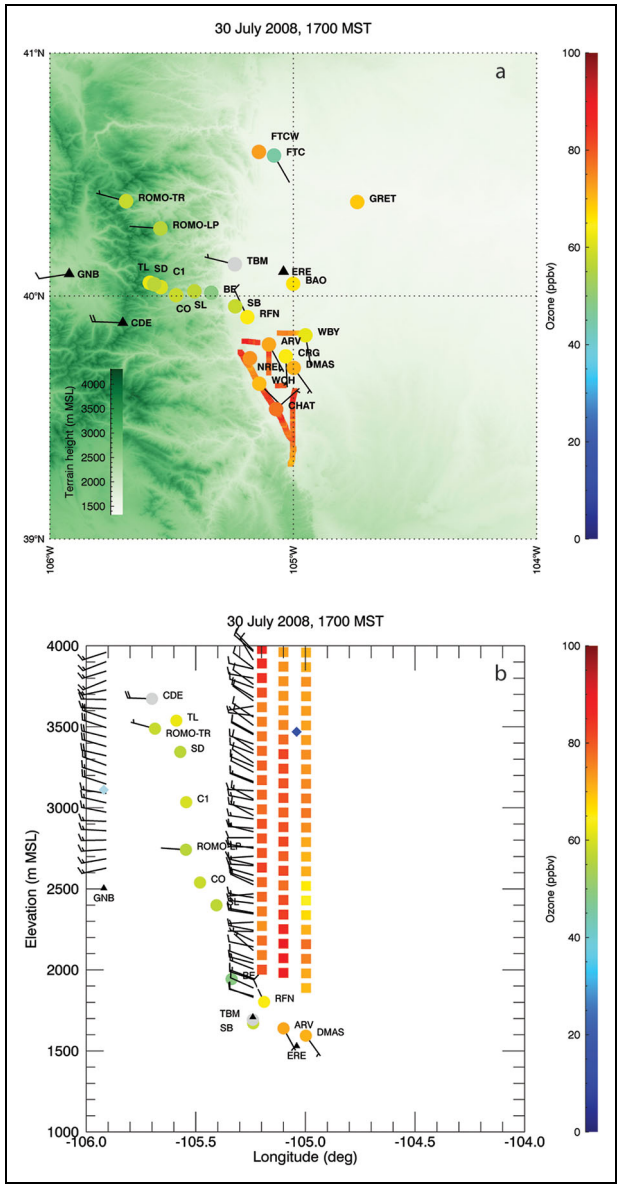


**Figure 8.** Plan view and height–longitude plots of hourly averaged ozone and winds. Same as **Figure 6** except for July 30 at 17:00 MST. DOI: https://doi.org/10.1525/elementa.2020.00146.f8

(**Figure 6**). These plots illustrate the intrusion of air with greater ozone values into the foothills at station elevations below the mixing depth measured at TBM—the slope-array sites and the RMNP station ROMO-LP. Mountain stations with a station elevation greater than the mixing depths over the plains were still showing background, or close to background, ozone mole fractions (56–65 ppbv, **Figure 9b**), even though the winds over the plains were easterly above the indicated mixing depths.

The portion of the TOPAZ flight from 14:00 MST to 15:00 MST (**Figure 10a and b**) measured ozone over the DMA and to the north and east of the urban area, and vertically averaged profiles indicated greater ozone values aloft than at the surface. The middle TOPAZ profile seen in **Figure 10b** had a maximum ozone of 99 ppbv and an average ozone value of 74 ppbv, whereas the DMA surface values ranged from 64 to 72 ppbv. The mixing depths were just over 3,700 m MSL, and by this time all stations, even those above 2,700 m MSL, were measuring ozone values >85 ppbv, well above background ozone; the maximum of 91.8 ppbv at C1 was the maximum hourly averaged ozone measurement of the year 2008 at C1 (as shown in Figure S2). The TBM profiler showed easterly winds between 2.5 and 8.5 m $s^{-1}$ from 85° to 150° throughout the profile.

The Twin Otter flew along the NCFR between 15:00 MST and 16:00 MST (Figure S5), flying just east of the foothills. The maximum TOPAZ ozone values were at least 10 ppbv greater than what was measured at the DMA surface stations. All mountain stations indicated high ozone values, ranging from 83 at SD to 97 at TL (Figure S5), which was the maximum hourly averaged surface ozone measurement of the day throughout the network. These ozone values were well above the background ozone values measured on July 30. As shown earlier, the ozone measured at the surface was

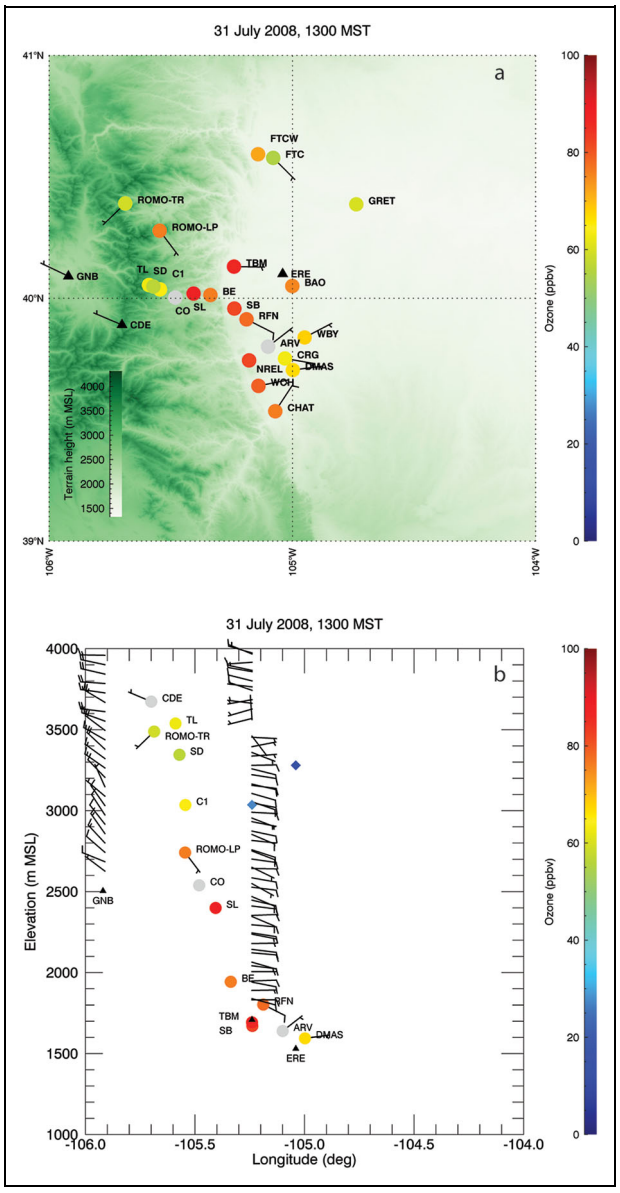


**Figure 9.** Plan view and height–longitude plots of hourly averaged ozone and winds. Same as **Figure 6** except for July 31 at 13:00 MST. DOI: https://doi.org/10.1525/elementa.2020.00146.f9

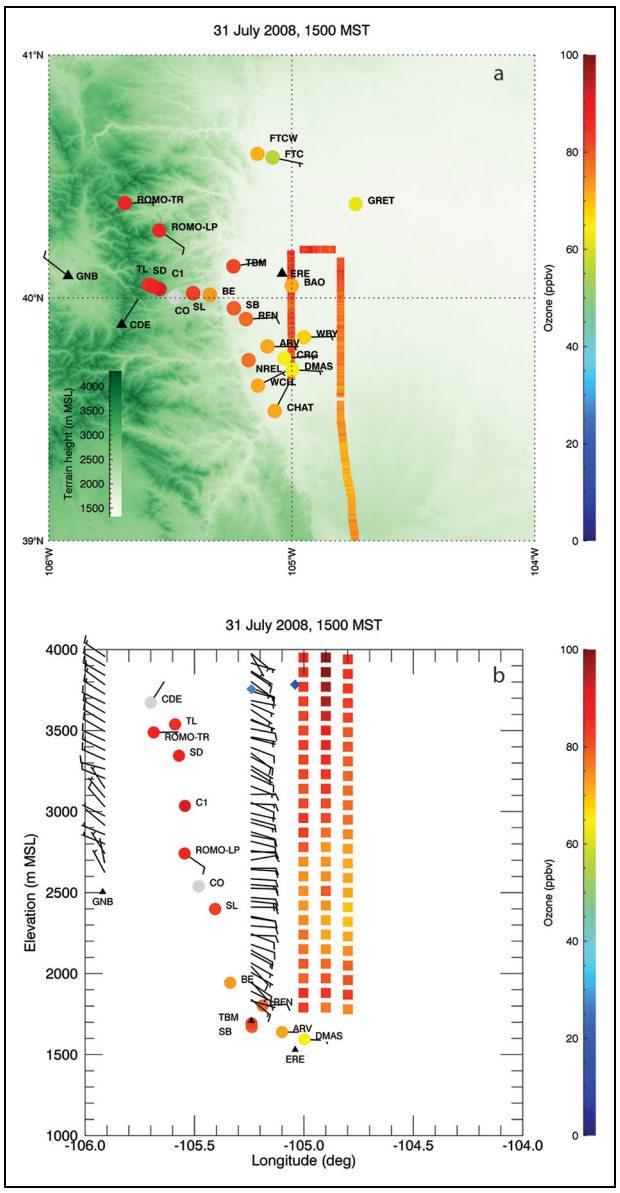


**Figure 10.** Plan view and height–longitude plots of hourly averaged ozone and winds. Same as **Figure 6** except for July 31 at 15:00 MST. DOI: https://doi.org/10.1525/elementa.2020.00146.f10

not necessarily representative of the ozone above the surface, where in this case, there was a deep reservoir of ozone-rich air as seen in the TOPAZ profiles. The Trail Ridge Road station (ROMO-TR), at 3,488 m MSL, is in RMNP. The ozone rose to 88 ppbv at ROMO-TR during this hour, the maximum ozone of the day at this station.

Between 16:00 MST and 17:00 MST (**Figure 11a and b**), the Twin Otter flew over the complex terrain of the Rocky Mountains and performed a partial box of ozone measurements around RMNP. The TOPAZ profiles over ROMO-TR and to the east indicated maximum ozone mole fractions of 100 ppbv. Ozone values to the northwest and west of ROMO-TR were lower, with a maximum ozone value of 65 ppbv in the flight leg north of GNB. The winds above 3,500 m MSL became southwesterly (235° at 0.25–7 m $s^{-1}$) during this hour. The mixing height at TBM reached almost 4,000 m MSL (2,300 m AGL), whereas at ERE, it continued its late afternoon descent to 2,700 m. Also, during this hour, ozone measurements had declined at the lower most slope stations (BE ozone fell from 76 ppbv at 13:00 MST to 61 at 17:00 MST and SL fell from 88 ppbv at 13:00 MST to 71 at 17:00 MST). Surface stations on the plains continued to measure easterly, upslope winds between 75° and 90° at 2 to 4 m $s^{-1}$. During the last hour of this TOPAZ flight (**Figure 12a and b**), the Twin Otter flew south to Granby (GNB), where ozone values were quite high, reaching 88 ppbv, then headed east, over more complex terrain and the slope array, to land near Boulder, CO.

19:00 MST to 20:00 MST was a transition time as sunset occurred at 19:15 MST. Daylight decreased, the mountain slopes cooled, and ozone production decreased, ending at

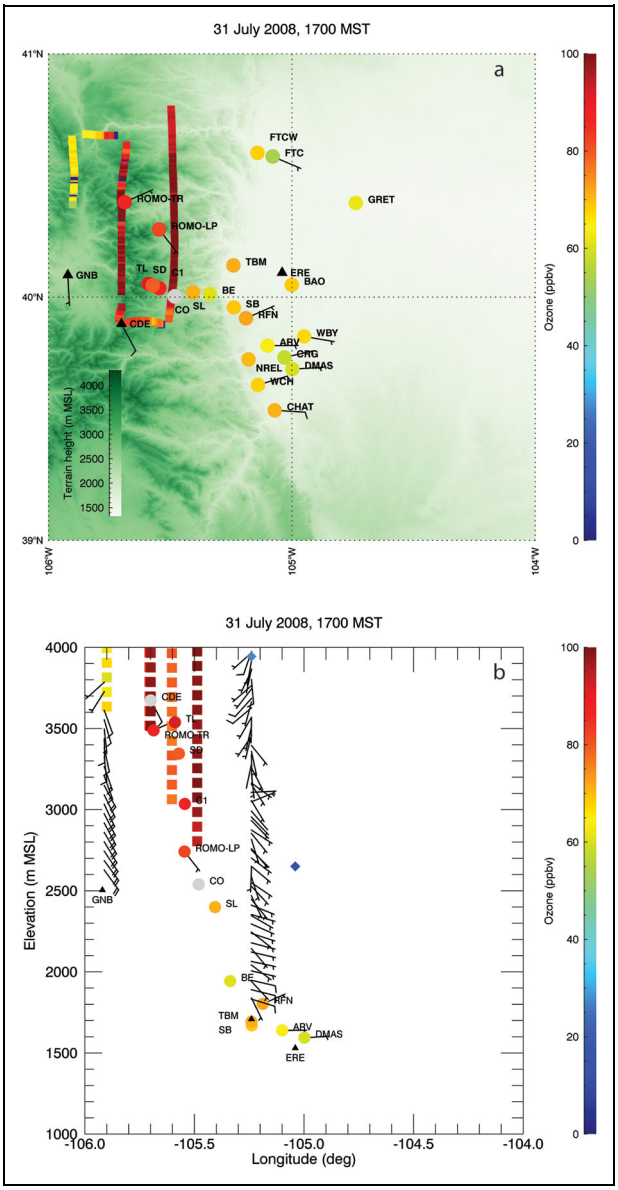


**Figure 11.** Plan view and height–longitude plots of hourly averaged ozone and winds. Same as **Figure 6** except for July 31 at 17:00 MST. DOI: https://doi.org/10.1525/elementa.2020.00146.f11

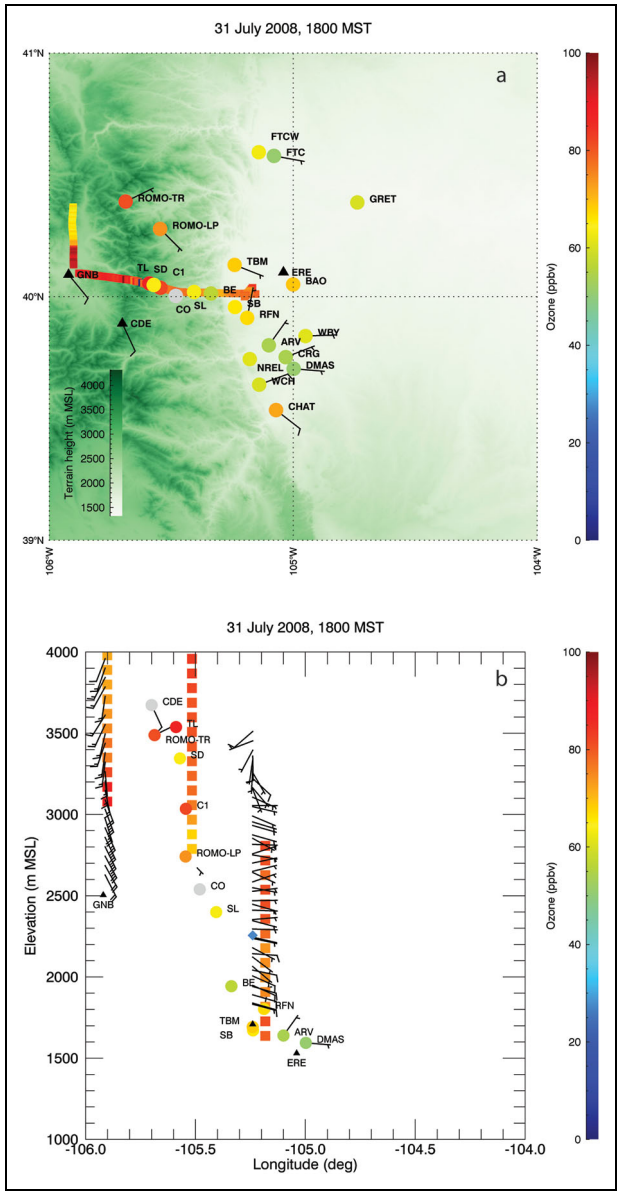


**Figure 12.** Plan view and height–longitude plots of hourly averaged ozone and winds. Same as **Figure 6** except for July 31 at 18:00 MST. DOI: https://doi.org/10.1525/elementa.2020.00146.f12

sunset. Katabatic westerly winds began, as seen in the lower 300 m of the TBM wind profiler data, and no well-defined convective mixing depths were measured (not shown). The mountain stations remained in easterly, upslope winds during this hour, as indicated by the TBM wind profiler winds (not shown).

At 22:00 MST (**Figure 13a and b**) TL, the ozone station at the highest elevation of all the surface stations continued to measure more ozone than any other surface station. However, at 71.5 ppbv, this was considerably lower than its maximum hourly averaged value of 97 ppbv at 16:00 MST. The wind profiler winds at TBM exhibited a transitional nature, with light winds from many directions, but downslope flow in the lowest 300 m was still discernable. By this time, the photochemical production of ozone had ceased.

## 5. Discussion

Our findings of efficient transport of ozone into and over the NCFR eastern Rocky Mountain foothills and the elevations of the Divide by thermally driven upslope flows under stagnant conditions coupled with a deep boundary layer are applicable to other regions where a large metropolitan area lies close to mountainous terrain.

For any metropolitan area near complex terrain, whether it is on the plains adjacent to a mountain range, such as the NCFR, or in a valley or basin, the pollution emitted will be subject to transport out of the region by winds that are driven by synoptic- or mesoscale meteorology. Each geographic region, such as Mexico City, Phoenix, Las Vegas, Los Angeles basin, Salt Lake City, or the San Joaquin Valley, will have its own unique geographic features defined by the height, complexity, and steepness of

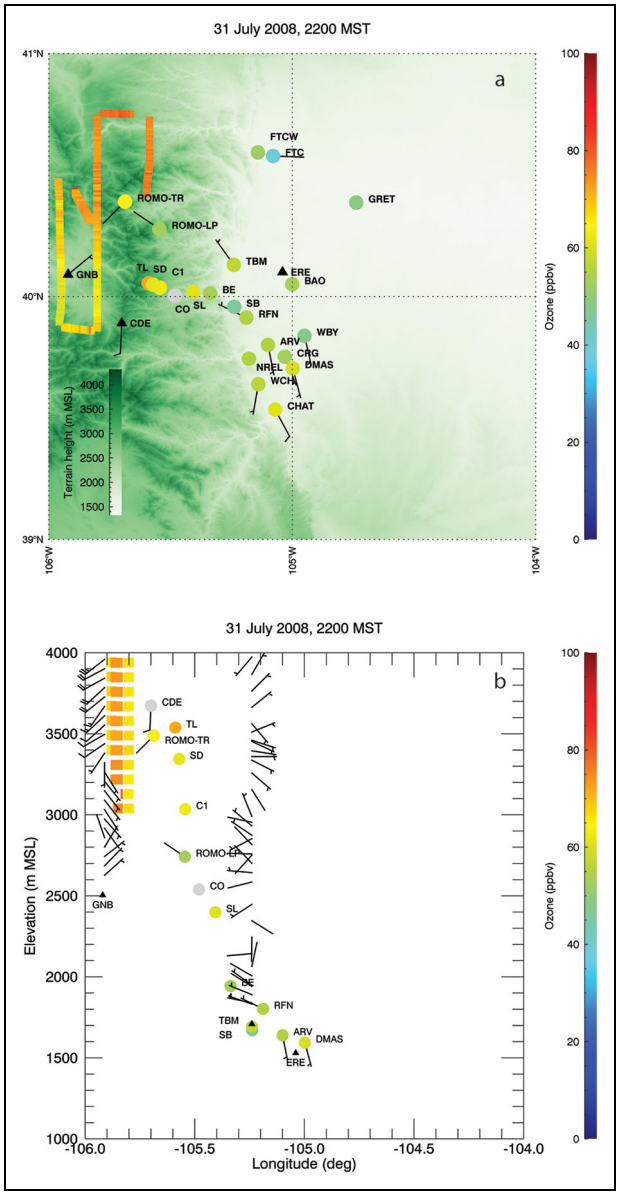


**Figure 13.** Plan view and height–longitude plots of hourly averaged ozone and winds. Same as **Figure 6** except for July 31 at 22:00 MST. DOI: https://doi.org/10.1525/elementa.2020.00146.f13

the nearby terrain, the timing of the maximum heating and cooling of nearby slopes, and vegetation type. These features will play a role in driving the mesoscale circulations that form there, as well as the effects of stronger, synoptically driven winds. Our analysis indicates that each setting will have its own combination of mixing depths and wind directions that will allow pollutants to accumulate, to be flushed out, or transported into mountainous areas. We note that mixing depths are a function of many factors including the synoptic-scale meteorology.

Transport of ozone into the adjacent mountains has been observed in the Los Angeles (Langford et al., 2010) and San Joaquin Valley (Fast et al., 2012; Panek et al., 2013) areas. Upslope transport of ozone into the Sierra Nevada in the Southern San Joaquin Valley often leads to poor air quality and high ozone concentrations in the Kings Canyon and Sequoia National Parks (east and southeast of Fresno, respectively), very similar to the conditions we observed in RMNP on July 31, 2008. However, poor air quality at these national parks tends to be confined to lower and mid-level mountain sites, whereas the air quality above 2,590 m tends to stay clean, regardless of air quality at the lower elevations (National Park Service—Sequoia and Kings Canyon Parks, 2021). Mixing depths in the Los Angeles Basin and especially in the San Joaquin Valley are quite shallow (Bianco et al., 2011) and well below mountaintop level. In the San Joaquin Valley, the shallow boundary layer heights are possibly due to cold marine air intrusion, irrigation, or subsidence over the valley due to mountain–valley circulations (Bianco et al., 2011). Therefore, ozone typically does *not* get transported up to and over the mountain ridges but rather is transported away from the mountain flanks toward the middle of the valley by the mountain–valley circulation (Fast et al., 2012; Panek et al., 2013). Langford et al. (2010) report on a case where ozone from the Los Angeles Basin was transported up the south-facing San Gabriel Mountains by the mountain chimney effect and injected into the lower free troposphere above the ridge of the mountains despite a mixed layer that stayed well below mountaintop level. However, no horizontal ozone transport over the mountain ridges and into the valleys beyond was observed, contrary to what we found in our case on July 31, 2008.

The orientation of the mountain ranges affects the timing and efficiency of the upslope ozone transport. For example, the south-facing San Gabriel Mountains in the Los Angeles Basin and the west-facing slopes of the Sierra Nevada get heated later in the day than the east-facing NCFR mountains. As result, the upslope flow attains its greatest strength at the time when ozone production peaks and the upslope flow persists longer into the afternoon and evening. This may have been the reason for the strong vertical ozone transport along the flanks of the San Gabriel Mountains reported in Langford et al. (2010), despite the rather shallow boundary layer depths.

Our July 31 case study day was a hot day with clear skies, little synoptic forcing, and a 500-mb ridge, perfect conditions for the formation of ozone, deep mixed layers, and the establishment of thermally driven slope flows that transported ozone and its precursors into the mountains west of the DMA/NCFR. Wind roses for 700 hPa (near mountaintop) for the summer of 2008, extracted from Denver radiosondes, and the Continental Divide winds at CDE for the time the meteorological station was running, show the relative rarity of east winds at these heights during the summer—the wind roses indicated that east winds at mountaintop height occurred approximately 7% of the time over the summer of 2008 (Figure S6). Gebhart et al. (2014) analyzed Front Range winds for a year (November 2008 to November 2009), sectioned by location. They found that east winds in the Northern Mountains and Northern Front Range (their geographical categories west and east of RMNP, respectively) occurred 6%–7% of the year, indicating that easterly winds at the high-elevation Rocky Mountain stations are rare year round.

The unique combination of measurements shown here brings a spatial coverage not normally available from the standard ozone monitoring in and surrounding the NCFR. Our analysis confirms previous analyses of elevated ozone events in the mountains west of the NCFR and west of the Continental Divide, associated with upslope flows. TOPAZ ozone profiles showed more horizontal and vertical coverage than previously published airborne in situ flight-level ozone data.

Our results indicate challenges for both forecasting ozone events for rural mountain stations and regulatory issues. According to the latest Colorado State implementation plan for the DMA/NCFR ozone nonattainment area (Colorado Air Quality Control Commission/Regional Air Quality Council, 2020), emission reduction measures include forecasting ozone exceedances more than 1 day ahead as part of the public outreach strategy, giving the public time to prepare to carpool or use public transportation on high ozone days. This will be a challenge for forecasting high ozone in mountain communities. Benedict et al. (2019) found that mesoscale modeling may underestimate the prediction of these upslope flows that transport ozone to the mountain elevations, one aspect of the general complexities associated with numerical modeling in the complex terrain of the NCFR.

As Oltmans et al. (2019) point out, the rural mountain areas are not included in the state's regulatory ozone monitoring (i.e., the CDPHE network of monitors). However, the CDPHE does include the RMNP observations as part of the regulatory monitoring. This still leaves a region of populated mountain communities south of RMNP, in and near the nonattainment area, which do not have regulatory monitoring. The highest elevation station in the CDPHE network is NREL, near the foothills at 1,830 m MSL. This NREL station is one of four stations near the foothills in the CDPHE network that are most likely to not meet the NAAQS 8-h ozone standard and is the one station that is projected to be out of compliance in the future (Colorado Air Quality Control Commission/Regional Air Quality Council, 2020). Thus, the residents of nearby mountain communities may be subjected to peak ozone events during the summer, when ozone can exceed regulatory surface station measurements on the plains, as in the present case. This brings up the question of whether the regulatory network should be expanded into mountain communities to protect citizens.

Although this analysis focused on the transport of ozone into the mountains, a similar effect is anticipated with westerly winds, when areas to the east of the NCFR would be affected. The TOPAZ ozone measurements in this region on July 30 presented a situation similar to the transport into the mountains on July 31 described here, in that ozone >80 ppbv was measured in the outflow from the NCFR/DMA, but this time over the eastern plains of Colorado, and again, outside of the regulatory network. The lack of ozone measurements on the eastern plains makes it close to impossible to assess the frequency of those occurrences and the resulting ozone exposure of communities in Eastern Colorado. Although those areas have relatively low population density, they are important agricultural production regions. These results open up questions about rural mountain and eastern plains communities' exposure to high ozone and possible negative health effects as well as the well-known damaging effect of ozone on vegetation, especially crops, perhaps leading to production losses to agricultural industries.

## 6. Summary

We have shown unequivocally that a deep, convective layer of ozone having values greater than 80 ppbv, at times up to 100 ppbv, existed over the plains, east of the Rocky Mountains, adjacent to the complex terrain of the foothills of the Rocky Mountains on both of our case study days. Although both days analyzed had deep mixing depths, at times close to mountaintop height, and TOPAZ profiles indicated high amounts of ozone in the boundary layer, the areas of high ozone exposure in the high-elevation rural mountains depended on the wind direction throughout the boundary layer for each day. This is consistent with previous studies along the NCFR that document greater ozone values at mountain stations with upslope flow and lower ozone values during times of downslope, westerly winds (Brodin et al., 2010; Pfister et al., 2017; Benedict et al., 2019; Flocke et al., 2019; Oltmans et al., 2019).

The CU slope array of ozone measurements west of Boulder, integrated with measurements from NOAA long-term monitoring stations, clearly showed the westward (and upward) creep of ozone values >90 ppbv into the NCFR foothills on July 31, transported by easterly winds beginning in the morning. The easterlies and mixing depths deepened through the day, transporting ozone to higher and higher elevation stations, until afternoon ozone levels at mountain stations exceeded background ozone and plains stations ozone. Presumably, ozone precursors were also advected toward the mountains and ozone was also produced aloft during this transport (Fehsenfeld et al., 1983; Oltmans and Levy 1994; Benedict et al., 2019; Oltmans et al., 2019). By evening, downslope flow formed, and ozone amounts began to decline.

On 31 July, the greatest hourly averaged ozone value recorded for the day at the surface stations analyzed, 97 ppbv, was measured at the highest elevation station (TL, 3,538 m MSL), and the greatest surface ozone value of the year at C1 (elevation 3,035 m MSL) was measured (Figure S2). Previous papers that assessed the source of pollutants in the NCFR (e.g., Cheadle et al., 2017; Pfister et al., 2017; Bien and Helmig, 2018; Benedict et al., 2019; Evans and Helmig, 2019; Flocke et al., 2019; Oltmans et al., 2019) indicate that oil and gas production east of RMNP contribute significantly to the NCFR regional ozone production. Consequently, it is likely that ozone resulting from oil and gas emissions could have been a factor in the amount of ozone precursors available for transport on our case study days.

The transport of ozone and its precursors to the high-elevation mountain stations did not end at these stations or at the Continental Divide. TOPAZ ozone measurements showed a continuous deep layer of high ozone values along the Divide. Pfister et al. (2017) and Flocke et al. (2019) also documented ozone "spillover" during Front Range Air Pollution and Photochemistry Éxperiment

airborne missions in 2014, and in the case of Pfister et al. (2017), their mesoscale modeling also indicated the advection of ozone across the Divide.

Although in different regions of the country, there are differences in the strength, timing, and spatial extent of upslope transport depending on local and regional conditions. Our findings highlight a process that is likely to be an important ozone transport mechanism in mountainous terrain adjacent to ozone source areas, when the right circumstances come together, namely a deep layer of light winds toward a mountain barrier together with a deep regional boundary layer. As we have shown, under these conditions, even tall mountain ranges may not act as natural barriers against pollutant transport. This has important ramifications for the health and well-being of people who live in rural, mountainous areas near large metropolitan areas.

## Data accessibility statement

Several of the data sets presented in this article can be found online:

NOAA/Global Monitoring Laboratory hourly ozone data are available online (ftp://aftp.cmdl.noaa.gov/ozwv/SurfaceOzone/). In the directory structure for this data archive, Tundra Lab/TL data are found in the TUN directory, C1 data are found in the NWR directory, and BAO data are found in the BAO directory (McClure-Begley et al., 2014).

National Park Service hourly ozone and wind data are available online (https://ard-request.air-resource.com/data.aspx).

NOAA/Physical Sciences Laboratory profiler and surface meteorological data can be found online on the "inactive stations" page (https://psl.noaa.gov/data/obs/datadisplay/archive/InactiveSites.html).

National Centers for Environmental Prediction/National Center for Atmospheric Research Reanalysis data can be plotted/downloaded at https://psl.noaa.gov/data/gridded/reanalysis/.

Validated Colorado State ozone and wind data can be requested from cdphe.commentsapcd@state.co.us.

An FRAQ data archive has been set up for the PSL mixing depths, CU slope array ozone data, and the Colorado State quality-controlled ozone and wind data: ftp://ftp1.psl.noaa.gov/psd2/data/realtime/processed/FRAQ/.

The CSL TOPAZ data can be downloaded from https://csl.noaa.gov/groups/csl3/measurements/2008fraqs/.

## Supplemental files

The supplemental files for this article can be found as follows:

**Figure S1.** Map of Denver Metropolitan Area and Northern Colorado Front Range 8-h ozone nonattainment area. This nonattainment area was established by the EPA in 2004. The blue shading denotes the nonattainment area. Note the overlap with Rocky Mountain National Park (green shading near the NW corner of the map). This map was created by the Denver Regional Council of Governments (June 2004) and can be found in the Denver Metro Area & North Front Range Ozone Action Plan, approved by the Colorado Air Quality Control Commission in December 2008 (https://www.colorado.gov/pacific/sites/default/files/AP_PO_Denver-Ozone-Action-Plan-2008.pdf).

**Figure S2.** Ozone measurements at Niwot Ridge, Colorado (referred to as "C1" in the main article). Measurements are for the year 2008 (*x*-axis is UTC). The maximum ozone concentration of the year at C1 was measured at 14:00 MST on July 31 with a value of 91.8 nmol $mol^{-1}$. The next hour, a concentration of 90.1 nmol $mol^{-1}$ was measured. August 27 had a close match to the July 31 maximum, seeing 91.2 nmol $mol^{-1}$ at 17:00 MST. This plot was created on the NOAA/GML web site: https://www.esrl.noaa.gov/gmd/dv/iadv/graph.php?code=NWR&program=ozwv&type=ts.

**Figure S3.** Plan view of hourly averaged ozone and winds measured at the surface for July 31, 2008. (a) 00:00 MST and (b) 06:00 MST. The station circles represent hourly averaged ozone. If the station circle is gray then either the station did not measure ozone or the hourly averaged ozone value was missing for that hour. The wind barbs are half barb = 2.5 m $s^{-1}$ and full barb = 5 m $s^{-1}$.

**Figure S4.** Plan view and longitude–height plots of hourly averaged surface ozone and winds for July 31, 2008. (a) Same as in Figure S3 except for 09:00 MST. (b) Height–longitude plot of select stations seen in the plan view plot at 09:00 MST showing surface ozone and wind measurements, wind profiles, and mixing depths (blue diamonds). The wind barbs are half barb = 2.5 m $s^{-1}$ and full barb = 5 m $s^{-1}$.

**Figure S5.** Plan view and longitude–height plots of hourly averaged surface ozone and winds for July 31, 2008. (a and b) Same as in Figure S4 except for 16:00 MST.

**Figure S6.** Wind roses showing the magnitude of occurrence of wind direction. Wind direction is shown in increments of 20°, color-coded by wind speed in knots. (a) Using 700-hPa winds from rawinsondes launched from Denver between June 1 and August 31, 2008. 700 hPa is approximately mountaintop height for the Northern Colorado Front Range. Note that most of the time the winds at that level are from the northwest. Winds from the east ($\pm$ 10°), as detected on one of our case study days, July 31, 2008, occurred less than 7% of the time during summer 2008. (b) From the PSL surface meteorological station deployed on the Continental Divide for the Front Range Air Quality Study (July 3 to September 12). Consistent with the rawinsonde data, easterly winds occurred approximately 7% of the time at the Continental Divide.

## Acknowledgments

The authors gratefully thank the engineers and technicians who installed, operated, and maintained instruments and collected the data sets used in this study. In particular, they thank Scott Sandberg and Ann Weickmann for the TOPAZ lidar data; Scott Abbott, Tom Ayers, Clark King, and Jesse Leach for the wind profiler and surface meteorology stations at CDE, ERE, GNB, and TBM. They also thank Daniel Gottas for the quality-controlled wind profiler data. Janet Intrieri (NOAA/PSL) and Andrew Langford (NOAA/CSL) provided helpful comments on the article. The authors thank the anonymous reviewers for their comments that helped to improve the article.

## Funding

Funding for the collection of the lidar, wind profiler, and surface meteorology data sets used in this research was provided by NOAA CSL and PSL. The surface monitoring along the vertical transect was funded in part by a National Science Foundation LTER grant (Grant Number: DEB-9211776) as well as through NOAA and the Colorado Department of Public Health and Environment (CDPHE). DH's contribution was in part supported by a contract from Boulder County Public Health.

## Competing interests

DH is the Editor-in-Chief of the Atmospheric Science domain of Elementa. He was not involved in the review process of this article.

## Author contributions

Contributed to conception and design: LSD, CJS, RJA, RMB, LB, DH, ABW.

Contributed to acquisition of data: CJS, RJA, DH, ABW.

Contributed to analysis and interpretation of data: LSD, CJS, RJA, RMB, LB, DH, ABW.

Drafted and/or revised the article critically for important intellectual content: LSD, CJS, RJA, RMB, LB, DH, ABW.

Approved the submitted version for publication: LSD, CJS, RJA, RMB, LB, DH, ABW.

## References

**Alvarez II RJ, Senff, CJ, Langford, AO, Weickmann, AM, Law, DC, Machol, JL, Merritt, DA, Marchbanks, RD, Sandberg, SP, Brewer, WA, Hardesty, RM, Banta, RM**. 2011. Development and application of a compact, tunable, solid-state airborne ozone lidar system for boundary layer profiling. *Journal of Atmospheric and Oceanic Technology* **28**: 1258–1272. DOI: http://dx.doi.org/10.1175/jtech-d-10-05044.1.

**Alvarez II RJ, Senff, CJ, Weickmann, AM, Sandberg, SP, Langford, AO, Marchbanks, RD, Brewer, WA, Hardesty, RM**. 2012 June 25–29. *Reconfiguration of the NOAA TOPAZ lidar for ground-based measurement of ozone and aerosol backscatter*. Proceedings of the 26th International Laser Radar Conference, Porto Heli, Greece: 249–252.

**Banta, RM**. 1984. Daytime boundary-layer evolution over mountainous terrain. Part I: Observations of the dry circulations. *Monthly Weather Review* **112**: 340–356. DOI: http://dx.doi.org/10.1175/1520-0493(1984)112<0340:DBLEOM>2.0.CO;2.

**Banta, RM**. 1986. Daytime boundary-layer evolution over mountainous terrain. Part II: Numerical studies of upslope flow duration. *Monthly Weather Review* **114**: 1112–1130. DOI: http://dx.doi.org/10.1175/1520-0493(1986)114<1112:DBLEOM>2.0.CO;2.

**Banta, RM, Cotton, WR**. 1981. An analysis of the structure of local wind systems in a broad mountain basin. *Journal of Applied Meteorology and Climatology* **20**: 1255–1266. DOI: http://dx.doi.org/10.1175/1520-0450(1981)020<1255:AAOTSO>2.0.CO;2.

**Banta, RM, Senff, CJ, Nielsen-Gammon, J, Darby, LS, Ryerson, TB, Alvarez, RJ, Sandberg, SP, Williams, EJ, Trainer, M**. 2005. A bad air day in Houston. *Bulletin of the American Meteorological Society* **86**: 657–669. DOI: http://dx.doi.org/10.1175/BAMS-86-5-657.

**Banta, RM, Shun, CM, Law, DC, Brown, WOJ, Reinking, RF, Hardesty, RM, Senff, CJ, Brewer, WA, Post, MJ, Darby, LS**. 2013. Chapter 8, Observational techniques: Sampling the mountain atmosphere, in Chow, FK, De Wekker, S, Snyder, B eds., *Mountain weather research and forecasting*. Dordrecht, the Netherlands: Springer: 494.

**Benedict, KB, Zhou, Y, Sive, BC, Prenni, AJ, Gebhart, KA, Fischer, EV, Evanoski-Cole, A, Sullivan, AP, Callahan, S, Schichtel, BA, Mao, H**. 2019. Volatile organic compounds and ozone in Rocky Mountain National Park during FRAPPE. *Atmospheric Chemistry and Physics* **19**: 499–521. DOI: http://dx.doi.org/10.5194/acp-19-499-2019.

**Bianco, L, Djalalova, IV, King, CW, Wilczak, JM**. 2011. Diurnal evolution and annual variability of boundary-layer height and its correlation to other meteorological variables in California's Central Valley. *Boundary—Layer Meteorology* **140**: 491–511. DOI: http://dx.doi.org/10.1007/s10546-011-9622-4.

**Bianco, L, Wilczak, JM, White, AB**. 2008. Convective boundary layer depth estimation from wind profilers: Statistical comparison between an automated algorithm and expert estimations. *Journal of Atmospheric and Oceanic Technology* **25**: 1397–1413. DOI: http://dx.doi.org/10.1175/2008JTECHA981.1.

**Bien, T, Helmig, D**. 2018. Changes in summertime ozone in Colorado during 2000–2015. *Elementa: Science of the Anthropocene* **6**: 55. DOI: http://dx.doi.org/10.1525/elementa.300.

**Bossert, JE, Sheaffer, JD, Reiter, ER**. 1989. Aspects of regional-scale flows in mountainous terrain. *Journal of Applied Meteorology and Climatology* **28**: 590–601. DOI: http://dx.doi.org/10.1175/1520-0450(1989)028<0590:AORSFI>2.0.CO;2.

**Brodin, M, Helmig, D, Oltmans, S**. 2010. Seasonal ozone behavior along an elevation gradient in the Colorado Front Range mountains. *Atmospheric Environment* **44**: 5305–5315. DOI: http://dx.doi.org/10.1016/j.atmosenv.2010.06.033.

**Carter, DA, Gage, KS, Ecklund, WL, Angevine, WM, Johnston, PE, Riddle, AC, Wilson, J, Williams, CR**. 1995. Developments in UHF lower tropospheric wind profiling at NOAA's Aeronomy Laboratory. *Radio Science* **30**: 977–1001. DOI: http://dx.doi.org/10.1029/95RS00649.

**Cheadle, LC, Oltmans, SJ, Pétron, G, Schnell, RC, Mattson, EJ, Herndon, SC, Thompson, AM, Blake, DR, McClure-Begley, A**. 2017. Surface ozone in the Colorado Northern Front Range and the influence of oil and gas development during FRAPPE/DISCOVER-AQ in summer 2014. *Elementa: Science of the Anthropocene* **5**: 61. DOI: http://dx.doi.org/10.1525/elementa.254.

**Coggon, MM, McDonald, BC, Vlasenko, A, Veres, PR, Bernard, F, Koss, AR, Yuan, B, Gilman, JB, Peischl,**

**J, Aikin, KC, DuRant, J, Warneke, C, Li, SM, de Gouw, JA**. 2018. Diurnal variability and emission pattern of decamethylcyclopentasiloxane ($D_5$) from the application of personal care products in two North American cities. *Environmental Science & Technology* **52**(10): 5610–5618. DOI: http://dx.doi.org/10.1021/acs.est.8b00506.

**Colorado Air Quality Control Commission/Regional Air Quality Council**. 2020. State implementation plan for the 2008 8-hour ozone National Ambient Air Quality Standard, Ozone SIP Element. Available at 121820+Apdx12-C.pdf (egnyte.com). Accessed 20 February 2021.

**Colorado Department of Public Health & Environment (CDPHE)**. 2009. Colorado 2008 Air Quality Data Report. Available at https://www.colorado.gov/airquality/tech_doc_repository.aspx. Accessed 23 January 2021.

**Defant, F**. 1951. Local winds, in Malone, TF ed., *Compendium of meteorology*. Boston, MA: American Meteorological Society. Available at https://doi.org/10.1007/978-1-940033-70-9_54.

**Evans, JM, Helmig, D**. 2017. Investigation of the influence of transport from oil and natural gas regions on elevated ozone levels in the Northern Colorado front range. *Journal of the Air & Waste Management Association* **67**(2): 196–211. DOI: http://dx.doi.org/10.1080/10962247.2016.1226989.

**Fast, JD, Gustafson Jr, WI, Berg, LK, Shaw, WJ, Pekour, M, Shrivastava, M, Barnard, JC, Ferrare, RA, Hostetler, CA, Hair, JA, Erickson, M, Jobson, BT, Flowers, B, Dubey, MK, Springston, S, Pierce, RB, Dolislager, L, Pederson, J, Zaveri, RA**, 2012. Transport and mixing patterns over Central California during the carbonaceous aerosol and radiative effects study (CARES). *Atmospheric Chemistry and Physics* **12**(4): 1759–1783. DOI: http://dx.doi.org/10.5194/Acp-12-1759-2012.

**Fehsenfeld, FC, Bollinger, MJ, Liu, CC, Parrish, DD, McFarland, M, Trainer, M, Kley, D, Murphy, PC, Albritton, DL**. 1983. A study of ozone in the Colorado mountains. *Journal of Atmospheric Chemistry* **1**: 87–105. DOI: http://dx.doi.org/10.1007/BF00113981.

**Flocke, F, Pfister, G, Crawford, JH, Pickering, KE, Pierce, G, Bon, D, Reddy, P**. 2019. Air quality in the Northern Colorado Front Range Metro Area: The Front Range Air Pollution and Photochemistry Éxperiment (FRAPPÉ). *Journal of Geophysical Research* **125**: e2019JD031197. DOI: http://dx.doi.org/10.1029/2019JD031197.

**Gebhart, KA, Malm, WC, Rodriguez, MA, Barna, MG, Schichtel, BA, Benedict, KB, Collett, JL, Carrico, CM**. 2014. Meteorological and back trajectory modeling for the Rocky Mountain Atmospheric Nitrogen and Sulfur Study II. *Advances in Meteorology* **2014**: 1–19. DOI: http://dx.doi.org/10.1155/2014/414015.

**Gilman, JB, Lerner, BM, Kuster, WC, de Gouw, JA**. 2013. Source signature of volatile organic compounds from oil and natural gas operations in Northeastern Colorado. *Environmental Science & Technology* **47**(3): 1297–1305. DOI: http://dx.doi.org/10.1021/es304119a.

**Helmig, D**. 2020. Air quality impact from oil and natural gas development in Colorado. *Elementa: Science of the Anthropocene* **8**: 4. DOI: http://dx.doi.org/10.1525/elementa.398.

**Kalnay, E, Kanamitsu, M, Kistler, R, Collins, W, Deaven, D, Gandin, L, Iredell, M, Saha, S, White, G, Woollen, J, Zhu, Y**. 1996. The NCEP/NCAR reanalysis 40-year project. *Bulletin of the American Meteorological Society* **77**: 437–471.

**Kaser, L, Patton, EG, Pfister, GG, Weinheimer, AJ, Montzka, DD, Flocke, F, Thompson, AM, Stauffer, RM, Halliday, HS**. 2017. The effect of entrainment through atmospheric boundary layer growth on observed and modeled surface ozone in the Colorado Front Range. *Journal of Geophysical Research: Atmospheres* **122**: 6075–6093. DOI: http://dx.doi.org/10.1002/2016JD026245.

**Langford, AO, Aikin, KC, Eubank, CS, Williams, EJ**. 2009. Stratospheric contribution to high surface ozone in Colorado during springtime. *Geophysical Research Letters* **36**: L12801. DOI: http://dx.doi.org/10.1029/2009GL038367.

**Langford, AO, Senff, CJ, Alvarez II, RJ, Banta, RM, Hardesty, RM**. 2010. Long-range transport of ozone from the Los Angeles Basin: A case study. *Geophysical Research Letters* **37**: L06807. DOI: http://dx.doi.org/10.1029/2010GL042507.

**Letcher, TW, Minder, JR**. 2018. The simulated impact of the snow albedo feedback on the large-scale mountain–plain circulation east of the Colorado Rocky Mountains. *Journal of the Atmospheric Sciences* **75**: 755–774. DOI: http://dx.doi.org/10.1175/JAS-D-17-0166.1.

**McClure-Begley, A, Petropavlovskikh, I, Oltmans, S**. 2014. *NOAA Global Monitoring Surface Ozone Network. 1973–2014*. Boulder, CO: National Oceanic and Atmospheric Administration, Earth Systems Research Laboratory Global Monitoring Division. DOI: http://dx.doi.org/10.7289/V57P8WBF.

**McDuffie, EE, Edwards, PM, Gilman, JB, Lerner, BM, Dubé, WP, Trainer, M, Wolfe, DE, Angevine, WM, deGouw, J, Williams, EJ, Tevlin, AG, Murphy, JG, Fischer, EV, McKeen, S, Ryerson, TB, Peischl, J, Holloway, JS, Aikin, K, Langford, AO, Senff, CJ, Alvarez II, RJ, Hall, SR, Ullmann, K, Lantz, KO, Brown, SS**. 2016. Influence of oil and gas emissions on summertime ozone in the Colorado Northern Front Range. *Geophysical Research Letters* **121**: 8712–8729. DOI: http://dx.doi.org/10.1002/2016JD025265.

**National Park Service**. Air quality and meteorological data. Available at https://ard-request.air-resource.com/data.aspx. Accessed 23 September 2020.

**National Park Service**. Impacts of ozone on park vegetation: Park Air Profiles—Rocky Mountain National Park (U.S. National Park Service). Available at nps.gov. Last Accessed 30 January 2021.

**National Park Service**. Sequoia and Kings Canyon air quality information: Air quality information—Sequoia & Kings Canyon National Parks (U.S. National Park Service). Available at nps.gov. Accessed 8 February 2021.

**NOAA/Global Monitoring Laboratory data**. 2020. Available at https://www.esrl.noaa.gov/gmd/dv/data/. Accessed 23 September 2020.

**NOAA/Physical Sciences Laboratory**. 2020. *PSL surface meteorology instruments*. Available at https://www.esrl.noaa.gov/psd/data/obs/instruments/SurfaceMetDescription.html. Accessed 1 February 2021.

**Oltmans, SJ, Cheadle, LC, Johnson, BJ, Schnell, RC, Helmig, D, Thompson, AM, Cullis, P, Hall, E, Jordan, A, Sterling, C, McClure-Begley, A, Sullivan, JT, McGee, TJ, Wolfe, D**. 2019. Boundary layer ozone in the Northern Colorado Front Range in July–August 2014 during FRAPPE and DISCOVER-AQ from vertical profile measurements. *Elementa: Science of the Anthropocene* **7**: 6. DOI: http://dx.doi.org/10.1525/elementa.345.

**Oltmans, SJ, Levy, H**. 1994. Surface ozone measurements from a global network. *Atmospheric Environment* **28**: 9–24. DOI: http://dx.doi.org/10.1016/1352-2310(94)90019-1.

**Panek, JD, Esperanza, SA, Bytnerowicz, A, Fraczek, W, Cisneros, R**. 2013. Ozone distribution in remote ecologically vulnerable terrain of the southern Sierra Nevada, CA. *Environmental Pollution* **182**: 343–356. DOI: http://dx.doi.org/10.1016/j.envpol.2013.07.028.

**Pétron G, Karion, A, Sweeney, C, Miller, BR, Montzka, SA, Frost, GJ, Trainer, M, Tans, P, Andrews, A, Kofler, J, Helmig, D, Guenther, D, Dlugokencky, E, Lang, P, Newberger, T, Wolter, S, Hall, B, Novelli, P, Brewer, WA, Conley, S, Hardesty, RM, Banta, R, White, A, Noone, D, Wolfe, D, Schnell, R**. 2014. A new look at methane and nonmethane hydrocarbon emissions from oil and natural gas operations in the Colorado Denver-Julesburg Basin. *Journal of Geophysical Research: Atmospheres* **119**(11): 6836–6852. DOI: http://dx.doi.org/10.1002/2013JD021272.

**Pfister, GG, Reddy, PJ, Barth, MC, Flocke, FF, Fried, A, Herndon, SC, Sive, BC, Sullivan, JT, Thompson, AM, Yacovitch, TI, Weinheimer, AJ, Wisthaler, A**. 2017. Using observations and source-specific model tracers to characterize pollutant transport during FRAPPÉ and DISCOVER-AQ. *Journal of Geophysical Research: Atmospheres* **122**: 10510–10538. DOI: http://dx.doi.org/10.1002/2017JD027257

**Reddy, PJ, Barbarick, DE, Osterburg, RD**. 1995. Development of a statistical model for forecasting episodes of visibility degradation in the Denver Metropolitan area. *Journal of Applied Meteorology and Climatology* **34**: 616–625. DOI: http://dx.doi.org/10.1175/1520-0450(1995)034<0616:DOASMF>2.0.CO;2.

**Reddy, PJ, Pfister, GG**. 2016. Meteorological factors contributing to the interannual variability of midsummer surface ozone in Colorado, Utah, and other western U.S. states. *Journal of Geophysical Research: Atmospheres* **121**: 2434–2456. DOI: http://dx.doi.org/10.1002/2015JD023840.

**Regional Haze State Implementation Plan**. 2015. Colorado regional haze plan: 5-Year progress report, Appendix E, 2015. Available at https://www.colorado.gov/pacific/cdphe/regional-haze-plan. Accessed 23 September 2020.

**Roberts, JM, Fehsenfeld, FC, Liu, SC, Bollinger, MJ, Hahn, C, Albritton, DL, Sievers, RE**. 1983. Regularities in the composition of aromatic hydrocarbon measured at Niwot Ridge, Colorado. *Atmospheric Environment* **18**: 2421–2432. DOI: http://dx.doi.org/10.1016/0004-6981(84)90012-X.

**Rossabi, S, Hueber, J, Wang, W, Milmoe, P, Helmig, D**. n.d. Spatial distribution of atmospheric oil and natural gas volatile organic compounds in the Northern Colorado Front Range. *Elementa: Science of the Anthropocene*, submitted, in review.

**Schmidt, G, Ruester, R, Czechowsky, P**. 1979. Complementary code and digital filtering for detection of weak VHF radar signals from the mesosphere. *IEEE Transactions on Geoscience Electronics* **17**: 154–161. DOI: http://dx.doi.org/10.1109/TGE.1979.294643.

**Stull, RB**. 1988. *An introduction to boundary layer meteorology*. Dordrecht, the Netherlands: Kluwer Acadamic, Springer: 10–15. DOI: http://dx.doi.org/10.1007/978-94-009-3027-8.

**Sullivan, JT, McGee, TJ, Langford, AO, Alvarez II, RJ, Senff, CJ, Reddy, PJ, Thompson, AM, Twigg, LW, Sumnicht, GK, Lee, P, Weinheimer, A, Knote, C, Long, RW, Hoff, RM**. 2016. Quantifying the contribution of thermally driven recirculation to a high-ozone event along the Colorado Front Range using lidar. *Journal of Geophysical Research: Atmospheres* **121**: 10377–10390. DOI: http://dx.doi.org/10.1002/2016JD025229.

**Szoke, EJ, Weisman, WL, Brown, JM, Caracena, F, Schlatter, TW**. 1984. A subsynoptic analysis of the Denver tornadoes of 3 June 1981. *Monthly Weather Review* **112**: 790–808. DOI: http://dx.doi.org/10.1175/1520-0493(1984)112<0790:ASAOTD>2.0.CO;2.

**Toth, JJ, Johnson, RH**. 1985. Summer surface flow characteristics over Northeast Colorado. *Monthly Weather Review* **113**: 1458–1469. DOI: https://doi.org/10.1175/1520-0493(1985)113<1458:SSFCON>2.0.CO;2.

**White, AB**. 1993 January 17–22. Mixing depth detection using 915-MHz radar reflectivity data. Eighth Symposium on Observations and Instrumentation; Anaheim, CA, AMS, Boston: 248–250.

**White, AB, Darby, LS, Senff, CJ, King, CW, Banta, RM, Koermer, J, Wilczak, JM, Neiman, PJ, Angevine, WM, Talbot, R**. 2007. Comparing the impact of meteorological variability on surface ozone during the NEAQS (2002) and ICARTT (2004) field campaigns. *Journal of Geophysical Research: Atmospheres* **112**: D10S14. DOI: https://doi.org/10.1029/2006JK007590.

**How to cite this article:** Darby, LS, Senff, CJ, Alvarez II RJ, Banta, RM, Bianco, L, Helmig, D, White, AB. 2021. Spatial and temporal variability of ozone along the Colorado Front Range occurring over 2 days with contrasting wind flow. *Elementa: Science of Anthropocene* 9(1). DOI: https://doi.org/10.1525/elementa.2020.00146

**Managing Editor-in-Chief:** Steven Allison, University of California, Irvine, CA, USA

**Associate Editor:** Isabella Velicogna, University of California, Irvine, CA, USA

**Knowledge Domain:** Atmospheric Science Domain

**Published:** May 11, 2021 **Accepted:** March 18, 2021 **Submitted:** September 25, 2020



ELEMENTA Science of the Anthropocene

*Elem Sci Anth* is a peer-reviewed open access journal published by University of California Press.

OPEN ACCESS